4/19/2022

The investigation of animal burrows in levees

Using experimental data to develop a probabilistic model that aims to improve the efficiency of manual inspection of animal burrows on levees

JOHANNES IDSINGA 4719646

The investigation of animal burrows in levees

Using experimental data to develop a probabilistic model that aims to improve the efficiency of manual inspection of animal burrows on levees

by

Johannes Idsinga
Student number: 4719646

Delft University of Technology
April 2022

Thesis committee:	Dr.ir. R.C. (Robert) Lanzafame	TUDelft
	Ir. S.J.H. (Stephan) Rikkert	TUDelft

Preface

This report presents my additional thesis for my Master Hydraulic Engineering at the Delft University of Technology. The topic of this research is the use of spatial and geometric characteristics of vole and mole burrow systems to develop a model that aims to improve the efficiency of manual inspection of a levee slope. The data that forms the basis for this thesis has been retrieved from experiments carried out at the Living Lab Hedwige and Prosper Polder between October 2021 and February 2022.

I would like to thank my supervisors Robert Lanzafame and Stephan Rikkert for guiding me throughout this project and providing me with useful feedback and advice during the process of writing this report. They were always available for questions and completely arranged my travel to the experiment site to help conduct the experiments in February 2022, for which I'm very thankful. Furthermore, I would like to thank André Koelewijn and Vana Tsimopoulou who lead the experiments that formed the basis of this report and shared all their captured data and information with me. Finally I wanted to thank everybody who helped carrying out the excavations experiments on February 8th and 9th 2022.

Johannes Idsinga
Delft, April 2022

Summary

Animal-induced anomalies on a levee surface negatively affect the erosion-resistance of a levee, leading to rapid failure of the inner slope in case of overtopping and/or overflow during high water. Where active prevention techniques of burrows from large animals, such as muskrats, are applied in and around levees in the Netherlands, the identification of smaller burrow holes made by voles and moles and the evaluation of the severity of the damage rely solely on the assessment and experience of the levee inspector.
The Polder2C's project aims to quantitively assess the impact of animal burrows on the levee surface by conducting experiments at the Living Lab Hedwige and Prosper Polder (LHPP) and this thesis aims to contribute in this by analyzing the experiment results and developing a model for levee inspection that includes uncertainties of the geometrical characteristics of vole and mole burrow systems.

This thesis distinguishes two phases, the first of which focuses on the question: 'How do animal burrows influence levee performance?', and it aims to form a foundation for the second phase of the report by focusing on the behavior of burrowing animals and the geometrical characteristics of their burrows by conducting a literature review on existing research on this topic. Guidelines were set up that contribute to the identification of mole and vole burrow system by investigating the main differences between them, with the aim to easily identify separate burrow hole groups in the experiment data. It was found that the levee surface area that is covered by the burrow hole group is the main parameter that sets apart a mole burrow system from a vole burrow system, with the threshold value being around 20 m^2. Any burrow hole group that covers a smaller area can be identified as a vole burrow system. For values between 20 m^2 and 90 m^2, other factors should be taken into account. These are the amount of burrow holes per m^2, higher values mean a higher probability of a vole burrow system being present, and the linearity in the distribution of the burrow holes. Moles are found to create longer, linear corridors where vole burrow system characteristically show a more random burrow hole pattern around the centrally located vole nests.
These conclusions could then be used to identify different vole and mole burrow hole groups in data that was collected from several experiments at the Living Lab Hedwige and Prosper Polder (LLHPP) between October 2021 and February 2022 and answer the research question for the second phase, which was: 'Based on data from levee inspection experiments, which probabilistic model can assess the inspection success rate of animal burrows?'. The process of these experiments have been elaborated on in chapter 4 and during the analysis of the experiment data in chapter 5, it was concluded that smoke experiments can potentially serve as a quick and effective method to gain insights in the connectivity between burrow holes and discover new burrow holes that are otherwise hard to discover by the naked eye. Furthermore, a vole burrow system was identified in the top-left part of the 4 meter wide levee stretch where the experiments were conducted consisting of 24 of the 93 burrow holes that were found in total. The remaining burrow holes are all expected to belong to the same mole burrow system.

The characteristic of these burrow system regarding the spatial distribution have been used to develop a probabilistic model, described in chapter 6, that will predict the responsible animal species that created the burrow and give a probability that describes the quality of the inspection. The model generates random burrow holes distributions within the input surface area based on the probability distribution functions that describe the smallest distance from a burrow hole to the nearest burrow hole from the experiment data, counts the average amount of burrow holes that appear in the generated burrow hole distribution and compares it with the input amount of burrow holes. In case a large discrepancy is found between the expected amount of burrow holes in the surface area from the generated burrow hole distributions and the actual amount of burrow holes found, the inspector could decide that further manual inspection of this levee stretch is desirable as he/she probably missed a lot of burrow holes.

Analysis performed on the experiment data suggests that a Gumbel distribution best fits the nearest-burrow distribution data in both vole and mole burrow systems. More specifically, it was concluded that the probability density function for the shortest distance from a vole burrow to the nearest vole burrow can be described by a Gumbel(μ=0.21,β=0.19) distribution and the probability density function for the shortest distance from a mole burrow to the nearest mole burrow can be described by a Gumbel(μ=0.34,β=0.21) distribution. Where μ is the location parameter and β is the scale parameter.

In addition to this, a logistic regression model is developed in order to identify the responsible burrowing animal taking more parameters into account than was originally done in the probabilistic model. These parameters were, besides the surface area and burrow hole density, the factor β which describes the 'slenderness' of the surface area and thereby taking the linearity in burrow hole distribution into account, where $\beta=1-\frac{\min(Height,Width}{\max(Height,Width)}$. Lastly, the value of r^2, with r being the correlation coefficient of a linear regression fit through the burrow holes, is taken into account when identifying the burrowing animal. This parameter also acts an indication of how well all the burrow holes fit on one line, high values for β and r^2 both hint towards mole burrow systems. The logistic regression model then takes a weighted average of the binary classification probability for each parameter, if a value of 0.5 or higher is found, a mole burrow hole is identified. In this way, inspectors can get a quick insight into the responsible burrowing animal and he/she can take further action.

All in all, it is concluded in chapter 7 that, while these models can be used as a first guideline towards improving the efficiency of manual inspection of a levee surface it has to be mentioned that most of the guidelines on which the models are based originate from a small amount of data. This brings limitations in the reliability and applicability of the models and therefore it is recommended that additional experiments should be carried out to increase the amount of data regarding the spatial distribution of vole and mole burrow holes and thereby verifying or adjusting the assumptions that were made during the development of the probabilistic model and the logistic regression model. Moreover, the amount of data should be increased in order to be able to accurately fit distribution functions through the nearest burrow histograms for the initial probabilistic model and to fit a logistic function through the binary classification graphs for the logistic regression model. Chapter 7 finally gives a recommendation on how to improve the efficiency of the experiment, where the main conclusions are that the use of a consequent local coordinate grid will greatly simplify the processes during the conduction of the experiments in the field as well as the processing of the data afterwards. In this way, the different detection methods that were tested during the experiment can be compared and their accuracies can be assessed which can provide useful information towards quantification of the effect of animal-induced levee anomalies in the future.

Table of Contents

Chapter 1: Introduction

1.1 Problem analysis and objectives

Anomalies in a dike, such as vegetation and animal burrows, negatively affect the levee resistance (Cobos-Roa, 2015). However, it is currently not taken into account in levee design and assessment (Palladino, 2019). The Polder2C's project is investigating the impact of these burrows of different animals on levee stability by carrying out experiments at the Living Lab Hedwige and Prosper Polder (LLHPP). History has shown that animal-induced anomalies strongly reduce a levee's performance in various ways and can even lead to failure of the levee. An example of this is the breach of an American levee in 2008 caused by muskrat burrows, where heavy seepage was recorded in a stretch of dike where these burrows had been found in the past. The combination of this seepage with landslide slope failures caused by collapse of these muskrat burrows ultimately lead to a breach (Bayoumi & Meguid, 2011). In addition, the identification of burrow holes and the risk evaluation from the presence of smaller animal burrows on the levee slope caused by voles and moles fully depends on the individual assessment of the inspector during manual inspection (Tsimopoulou & Koelewijn, 2022), while active measures exist to prevent damage caused by large burrowing animals such as the beaver or the muskrat (Hoogheemraadschap De Stichtse Rijnlanden, 2020). Further research on small animal burrows on a levee slope is necessary in order to improve detection methods, include the effect of these burrows in levee design and analyze and improve the efficiency of preventive measures and repairs.

This thesis will focus on the spatial distribution of vole and mole burrow holes along a dike stretch and the connectivity between these burrow holes and the main goal is to develop a model for levee inspection that includes uncertainties of the geometrical characteristics of the burrow systems. The report hereby mainly focuses on the identification of vole burrow systems and mole burrow systems and the differences between them, as they are more difficult to detect and show almost identical characteristics upon inspection.

Furthermore, the applicability of different burrow investigation techniques that have been tested during experiments at the LLHPP are assessed, so that the efficiency of manual inspection of a levee stretch can be improved. In order to do so, 2 phases can be distinguished within the project. The first phase consists of a literature study which focuses on getting a better understanding of the burrows and the animals that create them.

In the 2nd phase, the gathered data from all experiments is collected into one map, and the useful information is analyzed to investigate the geometrical characteristics of the animal burrows. Eventually a probabilistic analysis is carried out from which a model is developed that can be used in the future, as this model aims to identify the animal burrows and quantify the accuracy of manual inspection based on the uncertainties in geometrical characteristics of the burrows from the literature study and the experiment data.

1.2 Research topic

The research question for the first phase is:

- RQ1) 'How do animal burrows influence dike performance?'

which is composed of the following sub-questions:

- RQ1a) Which aspects of levee performance are altered by the presence of animal burrows?
- RQ1b) What are the characteristics of animal burrows in dikes?
- RQ1c) Which animals create burrows in dikes and why?
- RQ1d) What is the relation between the burrow entrance on the dike surface and the burrow system inside the dike?
- RQ1e) What are the parameters that determine the amount and distribution of burrows in a dike?

The research question for the second phase reads:

- RQ2) Based on data from levee inspection experiments, which probabilistic model can contribute to the manual inspection of animal burrows?

with the following sub-questions:

- RQ2a) What different measurement techniques for the investigation of dike burrow distribution and connectivity were tested during the experiments at the LLHPP?
- RQ2b) Based on data from experiments, which of these techniques can attribute to improved inspection of animal burrows on levees?
- RQ2c) What conclusions regarding the distribution of burrow hole entrances and their geometric characteristics can be drawn from the experiment data?
- RQ2d) What probabilistic model can be used to identify the burrow system and improve the efficiency of manual inspection of a levee slope?

1.3 Research Approach

This chapter describes the research approach that is used to answer the various sub-questions. The first phase, RQ1, is aimed to be answered qualitatively through performing a literature study of relevant sources. For RQ1a, reports on animal burrows in levees that have been written in the past will serve as a useful information source. RQ1b till RQ1e are closely linked through the behavior of the burrowing animals and therefore requires analysis of more ecological reports, which is especially the case for RQ1b and RQ1c. All in all, RQ1 aims to summarize the role animals play in levee performance and provide an overview on the characteristics of these burrows which could help identify animal burrow systems upon inspection and lay the foundation for the data analysis and probabilistic modelling in phase 2.

The sub questions that make up RQ2 are aimed to be answered based on data from several experiments which have been carried out using different detection methods. These experiments are first described and the data is collected into one map. The applicability of these methods for future experiments is assessed in RQ2b, based on the amount of data-processing that is required and the relevance/applicability of the data that is retrieved from these experiments.

After analyzing the geometrical characteristics of the vole and mole burrows that were found from the experiment data, a proposal for a probabilistic model that can be used to improve manual inspection is constructed which can help to identify the animal that created the burrow. Information on the characteristic size and spatial distribution of a burrow system from a certain species will be included in the model to help link the burrow system to an animal. This will be combined with geometrical characteristics of the burrows, retrieved from the experiment data to form a model that computes the expected amount of burrow holes in the manually inspected levee stretch and return a probability that at least one more burrow hole is present in the investigated levee stretch. For this, the model uses probability density functions fitted through the experiment data to generate random burrow hole distributions. In this way this model can be used to assess the accuracy of the inspection of the levee and help improve future levee inspection. The limited amount of data that is retrieved from the experiment lead to a poor fit of these pdf's in the model, which means that the applicability of the probabilistic model is limited as well. The model serves as a guideline for future research possibilities more than a definite tool for manual inspection of levees. Additionally, a logistic regression model is developed that uses four parameters regarding the size, burrow hole density and linearity of the burrow holes to identify a burrow hole group as either a mole or a vole burrow hole system.

Chapter 2: Investigating the effects of animal burrows on levee performance

This chapter aims to answer RQ1a, focusing on the way in which levee performance is negatively influenced by the presence of animal burrows based on available literature written on this topic. The failure mechanisms are described as well as the way animal burrows play a role in this.
It is not hard to imagine that the presence of animal burrows, nests and other holes have a negative impact on levee performance and that excessive burrowing can eventually lead to failure of the levee. Research from Van Baars (2009) has taught us that approximately 5% of the levee failures in the Netherlands between 1134 and 2006 has been caused by so-called '*External factors'.* It is mentioned that: *"These failures can be attributed to either humans or animals (…) for example rats or insects tunneling and burrowing* (Van Baars, 2009)*"*. It is mentioned that in total, 4% of levee failures are directly caused by animal burrows, so this excludes all the instances where animal burrows where present and could still be of influence but weren't the main cause of levee failure. Mitigation upon inspection and prevention of animal burrows in levee's can therefore be concluded to be of great importance, but exactly how do these burrows impact the levee?
There are multiple ways in which levee performance is reduced by the presence of these burrows, depending on the location of the burrows on the levee, the size of the animals that create them and the amount and distribution of the burrows. Three main categories can be distinguished, as described in the chapters below.

2.1 Change of the hydraulic characteristics of the levee

Burrow holes can change the phreatic surface inside the levee, for example when the protective clay layer is penetrated by an animal on the outer side of the levee or near the inner toe. Depending on the behavior of the animal this can be especially dangerous. For instance, beavers are known to dig burrows underneath the water line, leading to a relatively deep piercing of the clay layer. These burrow holes reduce the failure path through the aquifer, which is the permeable sand layer underneath the clay layer, and increases the pore pressures on the landside during high water. This will initially lead to uplift of the soil at the landside and eventually increases the probability of piping to occur. This is mentioned to be the greatest concern when considering the effects of animal burrows (FEMA, 2005).
Another way in which the hydraulic characteristics of the levee can be altered by burrow holes is that water can flow more easily into the core of the dike during high water and this raises the phreatic line within the levee. As a consequence, the levee saturation will increase and possibly micro-instability at the inner slope may occur with subsidence of the dike crest as a result. Furthermore, the increased phreatic lines can cause macro-instability of the inner slope, as the increase in pore pressures means a reduction in effective strength of the soil. Figure 1 from (Cobos-Roa, 2015) illustrates these aforementioned effects:

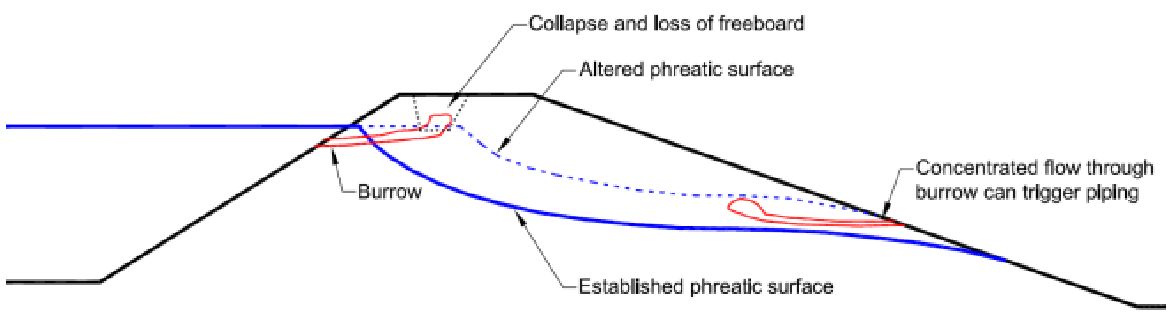

Figure 1: The influence of animal burrows on a levee's phreatic surface. Source: (Cobos-Roa, 2015)

While it can be concluded that the presence of animal burrows poses a significant threat to the performance of the levee, it has to be mentioned that these events will only take place in case of deep, large burrow that will extend deep into the levee body, for example created by large animals such as beavers or muskrats. More about the animals that create burrows can be found in chapter 3.

2.2 Reduction of erosion resistance

In case abundant burrow holes are present on the inner slope of the levee, the amount of erosion during overtopping is increased. The destruction of the grass cover means that progressively more subsurface soil is exposed to overtopping water which erodes the soil and removes it through the burrow holes. Experiments on this effect have been carried out by Koelewijn, Kieftenburg, Hûsken (2020) at the Living Lab Hedwige Prosperpolders where first a constant overflow discharge is applied on a 2 meter levee-stretch where no burrows are present. After 20 hours of testing with the maximum discharge of 350 l/s, no significant damage was reported. When the same or less overflow discharge was later applied to levee stretches where animal induced tunnels were present in the clay cover layer created by moles or foxes, the tests had to be stopped after only 1 hour due to the extensive damage to the dike slope (Koelewijn, Kieftenburg, & Hûsken, 2020). Figure 2 shows the damage at the location where mole tunnels were found and sand from the levee body is transported through some of these holes. Since the sand core at the Hedwige and Prosper polder is covered by a more erosion-resistant layer of clay, once this cover is removed and the flow reaches the sand core, the washout of the soil happens at a fast rate. This explains the large difference in result between the levee stretch with an undamaged clay cover and levee stretch with a penetrated clay cover. It also indicates the severity of the effects animal burrowing can have on levee performance.
It can be concluded that this effect of animal burrows is most likely to occur since even the smaller, shallow tunnels can have an influence.

Figure 2: Erosion damage at experiment site as a result of mole burrows, source: (Koelewijn, Kieftenburg, & Hûsken, 2020)

2.3 Reduction of crest height

Apart from subsidence of the levee crest through micro-instability, when multiple large sized burrow holes or networks are present in the levee, a local collapse of these large burrows can have the same consequence, with an increased possibility of more overtopping and/or overflow during high water as a result.

Chapter 3: Animal behaviour

This chapter aims to answer sub questions RQ1b and RQ1c, as it describes the types of animals that create burrows in levees in the Netherlands and their behavior. By investigating and summarizing the characteristics of the burrows created by each of these animals, the burrows can easier be classified upon inspection and a better view of the total burrow system within the dike can be achieved. Since burrows created by mole and mice are similar in location, entrance diameter and depth, more research on the geometrical characteristics of these animal burrows is done. In this way, the efficiency of the data analysis that is performed in chapter 5 can be improved which is linked to the probabilistic model that is constructed in chapter 6, which focuses on the identification of animal burrows on a levee surface.

Furthermore, examples are given from known burrow damage to levees so that the importance of burrow investigation is again underlined and burrow holes can be identified more easily in the field. Finally, the parameters that influence the presence and frequency of burrows are mentioned.

3.1: Types of burrowing animals

Burrowing animals are present in and around flood protections all throughout the Netherlands. In general, species that create burrows do so to create storage chambers for food or nests to raise and nourish their offspring. In the following subchapters, the most common burrowing species are described as well as the characteristics of their burrows.

3.1.1 Common vole (*Microtus Arvalis Pallas*)

The common vole is present throughout the whole of the Netherlands, mainly in grassland areas. Adult common voles can be between 10-12 centimeters long and around 4-5 centimeters in diameter. Their burrow systems are usually oriented parallel to the levee slope, while they occasionally dig straight down, with their nests usually at a depth of 15-30 centimeters and their tunnels reaching a depth of maximum 60 centimeters. The burrow system is characterized by tunnels leading from the burrow entrance holes on the slope of the levee to small chambers and nests where food is stored (Kennis- en Adviescentrum Dierplagen, 2022). Every 3-4 years a peak in the local 'mice cycle' is known to occur which in some cases can lead to a mice plague, causing damage to levees and grasslands, for example in 2014 in the province of Friesland (Deltares, 2014). In order for this peak in mice population to develop into a plague, it needs to occur simultaneously with exceptionally advantageous weather conditions the preceding months, namely a dry summer and autumn combined with a relatively warm winter. This is due to the fact that a small change in weather leading to unfavorable conditions (for example rainfall or cold temperatures during winter) will lead to stress among the mice population, resulting in mass mortality. Furthermore, sufficient food supplies and a low chance of predation needs to be present in order for a mice plague to develop (Provinsje Fryslân, 2015). Finally, mice plagues have

Figure 3: damage to levee as a result of a mice plague. Source: (Deltares, 2014)

historically been found to start in clayey/peat soils combined with a low water table. Figure 3 shows the damage to a levee slope as a result of this mice plague.
Regarding the geometrical characteristics of vole burrow systems, an interesting research has been carried out by (Brügger, Nentwig, & Airoldi, 2010) which contains data of 50 mole burrow systems in quasi-natural habitats and wild flower fields near Bern, Switzerland. Apart from the recorded data, some interesting findings have been made during this fieldwork. First of all, nests were found to be at central positions in all of the burrow systems, with different tunnels around it connecting to food storage chambers. It is further mentioned that each nest had an average of three entrances. The research found that in general, 3 types of burrow systems can be distinguished and the type of burrow system present is influenced by the habitat. The 3 types of system are: stretched out burrows with linear tunnels (type 1), dense and compact burrow (type 2) and burrows consisting of a mix of type 1 and type 2 (type 3). The report concluded that in wildflower fields dominated by grasses, burrow systems of type 2 were found to be more common. Quasi-natural habitats showed more type 1 systems. While it is unknown exactly what habitats are described as 'quasi-natural' habitats, the report does mention railway slopes mainly covered by grass as one of the investigated locations. Based on this, levee slopes could show similar results, with more stretched out burrow systems. However, since both types were found to be present at all 17 investigated locations, this conclusion might seem a bit premature (Brügger, Nentwig, & Airoldi, 2010).
Useful characteristics from the 50 analyzed burrow systems from (Brügger, Nentwig, & Airoldi, 2010) has been summarized in table 1:

Table 1: Average, minimum, and maximum values of parameters of 50 excavated vole burrow systems. Source: (Brügger, Nentwig, & Airoldi, 2010)

Parameters	Average value	Minimum value	Maximum value
System area (m^2)	7.5	0.5	28.8
Total tunnel length (m)	16.9	0.5	70.2
Tunnel density (m/m^2)	2.2	0.8	4
Tunnels deeper than 15 cm (%)	21.1	0	88.5
Min depth (cm)	5.7	2	11
Max depth (cm)	24.1	13	44
Average depth (cm)	12.6	7	23.4
Amount of nests	1.1	0	3
Amount of food chambers	0.8	0	5
Amount of burrow holes	17.2	2	58

Table 1 shows that vole burrows are generally characterized by a total surface area of maximum 30 m^2, with an average value of 7.5 m^2 and a relatively shallow depth of maximum 40 centimeter with an average value of 12.6 centimeters. Furthermore, a burrow system consists of 17 burrow holes on average. While all these values are based on one research and the values for these parameters are influenced by soil characteristics, food supply and other factors that might be different at the experiment site of LLHPP, these values do give an indication of vole burrow characteristics that can be used in comparison to mole burrow systems. This can help identify burrow hole system upon inspection and it can contribute to the construction of the probabilistic model in chapter 6.

3.1.2 European Water Vole (*Arvicola amphibius Linnaeus*):

This burrowing species' habitat is in and around the banks of rivers and ditches. The European water vole can grow to be between 16 and 22 centimeters long and excavate burrows that are characteristically slanted upwards from the bank into the soil, usually around 20 centimeters long and between 10-20 centimeters above the waterline. These burrows are usually connected by long 'corridors' running parallel to the waterline, at locations with many European water voles, these corridors can have a diameter of up to 15 centimeters. These tunnels often lead to food storage chambers of up to 50 centimeters to 1 meter depth (Kennis- en Adviescentrum Dierplagen, 2022).

3.1.3: Mole *(Talpa europea L.)*

Moles predominantly spend their lives underground. Moles usually have a solitary life and create individual burrow systems with the aim to trap as much prey as possible in the form of insects, larvae and earthworms. This explains why mole burrow systems are usually rather extensive, up to 70 meters long (YPTE, 2021). Tunnels have a diameter of approximately 5 centimeters and can vary in depth from close to the surface to a depth of about 70 centimeters (Bayoumi & Meguid, 2011). This depth of the mole burrow systems is found to be season dependent, as mole burrow system are usually located near the surface during summer. This is probably due to the fact that moles are able to find more food at shallower depth these months. As the winter approaches, food can mainly be found in deeper soil so mole burrow systems tend to be created at larger depths (Mellanby, 1971). Furthermore, research by (Haeck,1969) has mentioned that female moles tend to dig irregular tunnels where male moles usually build long, unbent tunnels with branches leading off it (Haeck, 1969). As more information regarding the geometric characteristic of mole burrows is necessary to better distinguish mole burrows upon inspection, research from (Haeck, 1969) is used to analyze the characteristic area and length of mole burrows. For this research, the burrows of 15 animals in the IJsselmeerpolder were monitored over the course of 5 years (from April 1960 till Jan 1965), and while the sample size might be a little small to draw definite conclusions, it does pose as a good indication of these parameters, which can be compared to information on vole burrows. The report mentions a mean average subterranean area of 490 m^2, with a minimum value of 92 m^2 and a maximum value of 2040 m^2, the total length of the tunnels that were found varied from 60 to 300 meters, with a mean value of 140 meters (Haeck, 1969). While the upper bound of these values seem too extreme for burrow systems in a levee, it can be concluded that mole burrow system can be identified based on their significantly larger dimensions compared to vole burrow systems.

3.1.4 Muskrat *(Ondatra zibethicus L.)*

The muskrats habitat comprises of basically anywhere with sufficiently deep and fresh water. The length of a muskrat can be up to 35 centimeters and the burrows created by them serve as a nest and have a relatively large diameter of 15-20 centimeters. The burrow entrance is typically located underneath the waterline and tunnels can penetrate all the way through the core of the levee body up to a depth of 3 meters below the water line. Muskrats are known to be aggressive burrowing animals, with one single muskrat being capable of removing 1 m^3 of soil per year (Bayoumi & Meguid, 2011). Due to the possibly disastrous consequences of muskrat burrows, Dutch law requires regional water authorities to protect their embankments from the damage coming from muskrat burrows (Hoogheemraadschap De Stichtse Rijnlanden, 2020). In practice this is done by placing traps, while newer technologies, like eDNA-detection and DNA mapping are currently in development as well (STOWA, 2022)

3.1.5 Beaver *(Castor fiber)*

Beavers can be found near rivers throughout the Netherlands and, as previously mentioned, are known to create burrows in banks of fresh water ditches near levees. Their burrow tunnels are usually between 30 centimeters and 2 meters deep and they create dens that can be several meters in diameter (Bayoumi & Meguid, 2011). Beavers can cause serious harm to a levee and therefore most regional water authorities make usage of certain ‘beaverprotocols’ to prevent beaver burrowing damage on levees (Waterschap Rivierenland, 2020).

3.1.6 Rabbit (*Oryctolagus cuniculus*)

Wild rabbits prefer half open landscapes like gardens and forests and usually live in extensive burrows consisting of multiple tunnels and nests where they live in families of maximum 10 rabbits. Occasionally, rabbits inhabit old foxholes and depending on the food supply in the area, the habitat of the rabbit is limited to the close vicinity of the burrow. The diameter of the tunnels is around 7.5 centimetres and rabbits are known to be sensitive to the saturation of the soil, a slight increase will lead to the rabbit family leaving its burrow in search of a more suitable location (Zoogdiervereniging, 2021).

3.1.7 Fox *(Vulpes vulpes L.)*

The habitat of foxes has expanded from mainly forest and dune areas to increasingly more urban areas. Foxes are territorial animals and they create fox holes or dens consisting of multiple tunnels where they raise their offspring. Moreover, the burrow systems are characterized by multiple entrances with a diameter of around 30 centimeters. In the previously mentioned report by (Koelewijn, Kieftenburg, & Hûsken, 2020), fox holes were found at one of the test sites and the effects of these burrows on the erosion resistance has proven to be disastrous. Figure 4 shows the damage from the experiments as a result of fox burrows.

Figure 4: Damage due to reduced erosion resistance from fox burrows. Source: (Koelewijn, Kieftenburg, & Hûsken, 2020)

The information from the various burrowing animal can be summarized into Table 1, which potentially can be used to distinguish the different burrow holes and network when encountered during levee inspection:

Table 2: Summary of burrow characteristics

Burrow entrance diameter	Entrance location	Burrow characteristics	Corresponding animal
3 – 5 centimeters	Levee surface	- Horizontal tunnel system leading to nests / storage chambers at 15-30 cm depth.	Common vole

		- Max tunnel depth of 60 cm	
3 – 5 centimeters	Levee surface	- Extensive amount of tunnels running all through the levee body - Max depth of 70 cm	Mole
< 15 centimeters	In and around fresh water banks	- Slanted tunnels from bank into dike body - Many chambers, with a max depth of 1 m, connected by corridors	European water vole
7,5 centimeters	Inner slope / inner toe	- Extensive amount of tunnels and chambers to house family	Rabbit
15-20 centimeters	In and around fresh water banks	- Tunnels penetrating all through levee body - Entrance depth can be up to 3 meters	Muskrat
15-20 centimeters	Underneath water line	- Tunnels leading to large dens of a few meter diameter - Depth of burrow system ranging from 30 cm to 2 meters.	Beaver
30 centimeters	On dike surface	- Multiple burrow entrances leading to dens	Fox

From table 2 it can be concluded that most animal burrows are quite distinct and can easily be identified based on either entrance diameter or entrance location or both. However, this is not the case for vole and mole burrows and since they are of great relevance for this report, which focuses on the inspection of the levee surface, additional comparison of the two burrowing species is necessary.

3.2: Vole versus mole burrow systems

As mentioned in chapter 3.1, mice and mole burrow system have similar characteristics. Burrow holes from all other species in table 2 can be recognized more easily in practice based on either the diameter and/or burrow hole location. However, since the burrow entrance diameter and location are similar among voles and moles, it might be hard to distinguish which animal is responsible for the burrow when such a hole is found during inspection of a levee stretch. This chapter aims to summarize the main differences between the geometric characteristics of the two burrow types, thereby answering RQ1d and serving as a foundation for the data analysis that is performed in chapter 5.2.
First of all, the main differences in burrow system between mice/vole and mole burrows result from the different behavior of the two species and the disparate purpose that the burrows have. Where voles use their burrows as a shelter to protect their offspring, their food and themselves from

predators, they usually look for food above the surface and bring this back to their subsurface chambers. This results in a burrow system consisting of multiple small chambers that are connected by corridors (Kennis- en Adviescentrum Dierplagen, 2022). Furthermore, the burrows are often built in one level only, parallel to the ground surface.
On the other hand, moles build their nest in dry spots in the subsurface and also use underground tunnels towards humid parts of the soil as a way to catch food. This leads to more extensive burrow systems, characterized by long tunnels with a total length of a few hundred meters (Mellanby, 1971).
Table 3 further summarizes these characteristics, based on research from (Brügger, Nentwig, & Airoldi, 2010) and (Haeck, 1969).

Table 3: Comparison of geometric characteristics of vole and mole burrows. Sources: (Brügger, Nentwig, & Airoldi, 2010) & (Haeck, 1969)

Parameter	Vole burrows	Mole burrows
Min. burrow system area (m^2)	0.5	92
Mean burrow system area (m^2)	7.5	490
Max. burrow system area (m^2)	28.8	2040
Min. total tunnel length (m)	0.5	60
Mean total tunnel length (m)	16.9	140
Max. burrow tunnel length (m)	70.2	300
Min. burrow depth (cm)	5.7	Unknown
Mean burrow depth (cm)	12.6	Unknown
Max. burrow depth (cm)	24.1	unknown

Even though this data is based on a small sample size, some useful conclusions can be drawn from table 3, as well as the other information from chapter 3.1:

- Burrow groups that span a surface area between 0 and 20 m^2 can be concluded to be vole burrows. Larger burrow areas are likely to be made by moles. In practice, it is unlikely to find all burrow entrances that are part of the mole burrow during inspection, as it can span across a large levee stretch. It is therefore easier to set this threshold with regards to vole burrow system and regard larger burrow groups to be (part of) mole burrow systems.
- Mice burrow systems can be recognized by a central nest, containing an average of 3 burrow entrances, connecting to multiple burrow holes in the near vicinity.
- An average of 17 burrow holes are found to be present in vole burrows, with an average surface area of 7.5 m^2, this leads to an average burrow hole density for voles of 2.3 burrow holes per m^2
- Burrow holes that extend to a depth of more than 30 centimeters can be concluded to be mole burrow entrances.

These conclusions can be used to identify burrow groups in the experiments data, as done in chapter 5.2.

3.3: Parameters of influence

The amount of burrow holes in a levee stretch are a function of a number of parameters. Logically, **the amount of available food sources** in the area is the main driver for a large burrow density, which is closely linked to **competition** between different species fighting for the same food source. Burrowing animal species can also form a food source for other species, which is why **the presence of predators** also influences the amount of burrowing species in an area.
Furthermore, the **soil type** plays an obvious role. Research from (Laundré & Reynolds, 1990) showed a positive correlation between the percentage of silty, clayey soil material and the size and density of burrows. On the other hand, an increasing amount of sandy soil reduced the size of the investigated burrows. This is not a surprising conclusion, since we know that sandy soils are stronger and harder

than clay and therefore impose a higher resistance for burrowing species. Furthermore, tunnel systems in sandy soils are more likely to collapse, explaining why species prefer a clayey soil type. In the Living Lab HedwigeProsperPolder, where the experiments described in chapter 4 took place, the levees consist of a sandy core with a clay cover of 30 to 80 centimeters (Koelewijn, Kieftenburg, & Hûsken, 2020), posing as a suitable location for shallow burrow systems created by relatively small animals like voles or moles as described in table 1.

Another crucial parameter in the amount and distribution of animal burrows is the **moisture content** of the soil which is related to the water table. If the soil is too dry and hard, species are less likely to dig extensive tunnels since they have a higher chance of collapse. On the contrary, in case of high water and increasing water table the soil will become too moist, posing a risk of drowning for the burrowing species. This results in burrows being created higher up the levee slope in case of high water (Bayoumi & Meguid, 2011).

Finally, the **extent of maintenance practices** including for example the trapping of the animals or the grouting of their burrows upon inspection is a parameter of influence for the amount of burrowing species near the levee. (Cobos-Roa, 2015).

Chapter 4: Experiment description

In this chapter, the experiments that are carried out at the LLHPP (Living Lab Hedwige and Prosper Polder) are described and the main objectives of these experiments are mentioned. The procedures of these experiments are described and illustrated with pictures.

All of the experiments that are described in this chapter were conducted at the Living Lab HedwigeProsperpolders (LLHPP), which is located on the left bank of the Scheldt and lies partly in Dutch and Partly in Belgian territory. Since this area is given back to nature in order to enhance the ecological conservation and development, the primary flood defenses are being removed and it serves as a perfect site to perform experiments (STOWA, 2022). For the series of experiments that are described here, involving the detection of (shallow) animal burrows, a levee stretch on the Prosperpolder of approximately 4 meters is used, figure 5 indicates this experiment location on a map (Google Maps, 2022). The soil profile of this part of the levee consists of a clayey sandy core with a layer of around 40-50 centimeters of slightly sandy clay (Koelewijn, Kieftenburg, & Hûsken, 2020).

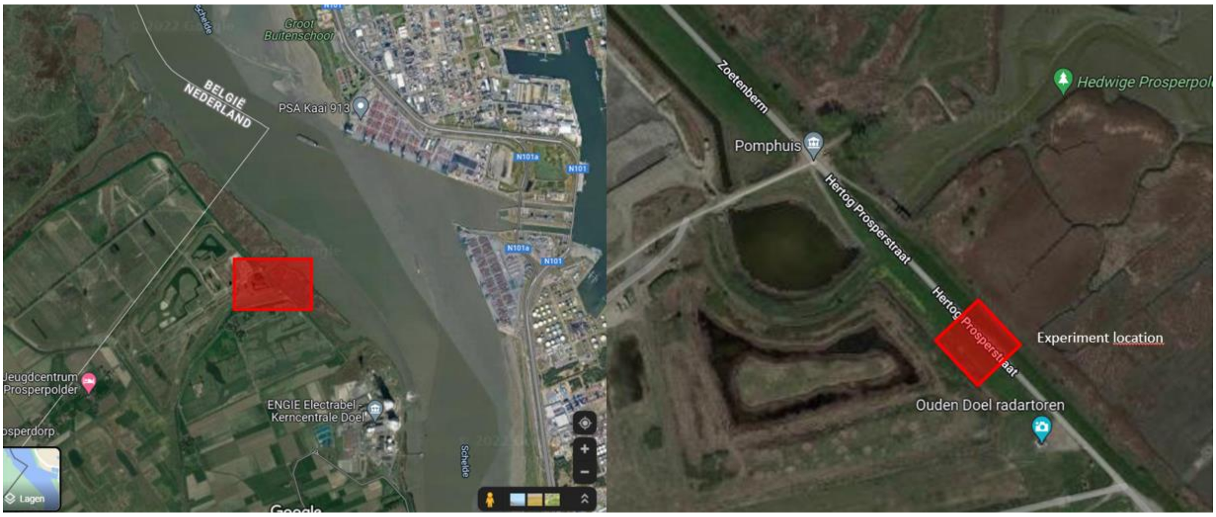

Figure 5: Experiment location, with the levee location (left) and the local levee stretch (right)

The experiments described in this report have been carried out in two phases: the grouting and smoke experiments (combined with some excavations) and GPR scanning of the burrow system were performed on the 6th, 7th and 9th of October 2021. Most of the (remaining) excavations as well as the RTK-GPS and LiDAR scans were carried out on the 8th and 9th of February 2022.

4.1 First experiment session (6th,7th, 9th of October 2021)

The first batch of experiments were carried out by a team of TU Delft and HZ University of Applied Sciences, in collaboration with Lille University (who were responsible for the GPR scans). Further details regarding the different experiments are given in the following subchapters.

4.1.1 Smoke Experiments

On the 6th of October 2021, smoke experiments were carried out on the 4 meter wide levee stretch, where smoke was blown into one of the burrow holes and every burrow hole in the vicinity that showed smoke coming out of the hole was marked. In this way, connected burrow holes can quickly be identified and an indication of the underlying burrow system can be made. The main goal of this experiment was to explore and assess the applicability and accuracy of this detection method. Additionally, this experiment aims to identify the interconnection of burrow holes on the levee slope and compare these results with the results from other experiments in order to get a total image of the burrow system.

The experiments were carried out in the following way. The smoke was created by diffusing a smoke ball and placing it in an empty barrel, which was connected to a rubber hose in one of its openings. A leaf blower was then quickly placed on top of the other opening, which forces the smoke through the rubber hose. The rubber hose was placed in one of the burrow holes and closed off by covering it with a layer of soil so that the smoke would indeed travel through the burrow. An image of this procedure is depicted in figure 6.
The vicinity of this burrow hole was then checked and every other hole that showed smoke was marked and filled up with soil until no smoke could be seen coming up from the levee slope. Figure 7 is taken from a demonstration of this method, in the background the smoke blowing installation can be seen and in the foreground this orange-colored smoke can be seen coming up from another spot.

Figure 6: Smoke experiment procedure, using a leaf blower, smoke is blown from the barrel, through the rubber hose, into the burrow hole

Figure 7: Demonstration of the smoke experiment. The red box indicates smoke coming up from a connected burrow hole

The coordinates of the burrow holes that showed smoke during these tests were later mapped, using the coordinate system that was also used during the GPR scan experiments.

4.1.2 GPR scanning

Ground penetrating radar (GPR) is a detection method which sends an electromagnetic signal into the soil and detects the reflected signals to identify the presence of different soil materials in the subsurface. These resulting scans indicate the differences between the electromagnetic properties of the existing materials and it can therefore be used to identify burrow systems since voids in the subsurface reflects this signal differently than the soil around it (GPRS, 2022). On the 7th of October 2021, a GPR scan was carried out on 2 zones of 2 by 4 meters, illustrated in figure 8. The aim of the experiment was to test the applicability of GPR test to identify burrow systems.
In order to accurately interpret the resulting scans, the complete levee stretch was divided into a grid of spaces with a width of 50 centimeters (in horizontal direction) and a length of 1 meter as visible in Figure 8.
Simultaneously, all burrow holes that were encountered on the grid were marked with color and a flag, see Figure 9, so that mapping of the burrow holes upon manual inspection was simplified.

Figure 8: Coordinate grid used for GPR scans

Figure 9: Marked burrow holes on the coordinate grid

Figure 10: The GPR scanning a section of the levee

4.1.3 Grout Experiments

By pouring grout into burrow holes and excavating this when the grout has solidified, the exact course of burrow system can be identified, which is the main goal of these experiments, carried out on the 7th of October 2021. Furthermore, the excavated burrow system can serve as a reference to assess the accuracy of the other detection methods. For instance, in case the GPR scan shows a certain burrow tunnel at one location, the excavated grout could confirm this and say something about the discrepancy in size or location of the tunnel in comparison to the GPR scan.

The burrow holes that were previously marked and identified on the same coordinate grid as used to make the GPR scans, were filled with a total of 20 liters of grout, spread over the 63 burrow holes that were found on this 4 meter wide stretch of the levee. Figure 11 shows the process of filling a burrow hole with the grout mixture and figure 12 indicates the final result, after all burrow holes have been filled up.

Figure 11: Filling a burrow hole with grout

Figure 12: Numerous grout-filled burrow holes on the coordinate grid

4.1.4 Initial excavations

During a small session of the winter school on October 9th, where students of the HZ University of Applied Sciences could get familiar with the LLHPP and participate in activities centered around the effect of animal burrows on the erosion resistance of levees, a few of the grouted burrow holes were excavated. The groups used garden tools to dig in the vicinity of the marked burrow holes to aim and follow the grouted system as accurate as possible. Most of the excavations took place close to the levee crest, see chapter 5 for a more detailed map. While plenty of pictures and videos were made of the experiments, unfortunately no data regarding the orientation of the excavated burrow system or other findings were saved. This means that no information is available regarding the extent and distribution of the burrow system of the excavated grouted elements.

Figure 13: Excavations during the winter school session on Oct 9th 2021

4.2 Second experiment session (8th and 9th of February 2022)

This batch of experiments was again carried out by a team from TU Delft, HZ University of Applied Sciences and Deltares. The following subquestions describe the procedure of the experiments that took place those two days.

4.2.1 Excavations

Similar to the excavations on October 9th, garden equipment was used to excavate a large part of the grouted burrow system, which was grouted during the first batch of experiments on October 7th. On the 8th of February, a group of approximately 10 people started digging out the grout around the marked burrow entrances. The unpredictable nature of the burrows made it relatively hard to accurately follow the burrow system through the soil and the fact that the grout became highly brittle and sometimes hard to distinguish from the soil with the naked eye, caused damages to the grouted burrows. In practice, grouted burrow parts were often found piece by piece and in most cases the trail was lost after a while. On the second day, the 9th of February, a smaller group of 6 people continued following the traces from the previous day and eventually, in 2 areas of the levee, intact burrow tunnels were found. One of which is located towards the toe of the levee, and connected to a large chunk of grouted material on top of the levee surface, this was a location were a lot of grout poured out during the grouting of the holes on October 7th. The tunnels that were found were relatively long, in the order of a few meters and consisted of branches, making up a tunnel system with a diameter of a few centimeters, characteristically made by moles. Images of this burrow system can be seen in figures 14 and 15. Further up the slope, towards the crest, a small system of dense tunnels was found, assumed to be connected by small chambers which is characteristically made by mice. The mole burrow system was later scanned by the LiDAR and the location of interesting points on the grouted system was measured using RTK-GPS scanning. In chapter 5, the results from these scans are treated.
The excavated burrows that are visible in Figure 15 are connected to those visible in Figure 14.

Figure 14: Part of the excavated mole burrows.

Figure 15: Excavated mole burrow system

Figure 16 shows the mice burrow system that is excavated near the levee crest.

Figure 16: Excavated mice burrow system

4.2.2 RTK-GPS scans

As previously mentioned, the coordinates of points of interest of the excavated burrow systems were scanned using Real Time Kinematic (RTK) measurements. RTK measurements use phase delays of signals between satellites to accurately determine the location of the rover. It returns the x, y and z coordinates in the Dutch Rijksdriehoek coordinate system, more on this can be found in chapter 5. The accuracy of the RTK locations are in the order of 1 – 2 centimeters (Utiugova, 2021).
Apart from the excavated burrow systems, the coordinates of some of the grouted burrow holes were scanned before the excavations took place. The aim of the RTK measurements is to determine these exact location and thereby to facilitate the mapping of the different datasets as well as to assess the accuracy of manual inspection and mapping of the burrow holes on the levee slope.
In some instances, the points of interest that were measured by the RTK were photographed and the measurements were given a name, so that the RTK measurements could be linked with the LiDAR scans. In practice, many of the RTK measurements were given unclear names that were impossible to link with the photos and in other instances no photos were taken at all. This resulted in the fact that

only a handful of pictures/measurements could be used for the registration of this data into the LiDAR scans, resulting in a lower accuracy of the alignment.

4.2.3 LiDAR scans

Light Detection and Ranging (LiDAR) scanners use lasers to evaluate distances and depth. Every laser scan creates one point and all of these millions of points combine into an accurate 3-dimensional image of the excavated burrow systems. In total, 4 different scans were made using the LiDAR scanner built into the iPad. The goals of these scans is to facilitate the mapping of the excavated areas.
Post-processing and analysis of these scans are made using the open-source software CloudCompare, the full scan of the total excavated area consists of approximately 7.5 million data points.

Chapter 5: Experiment results

In this chapter, the gathered data from the experiments that are described in chapter 4 are first collected and mapped in chapter 5.1, from which the areas of interest for further data analysis can be identified. In chapter 5.2, some initial conclusions on the burrow system and it's detection methods are made and chapter 5.3 assess the applicability and efficiency of the different detection method used during the various experiments.

5.1 Collection and mapping of data

The results from the various experiments are shown and eventually combined into one map, which serves as the foundation for the analysis of the burrow system. The method used to process the data is briefly explained and supported with images.

5.1.1 Grouting and Smoke experiments (7th and 8th of October 2021)

The local coordinates of all the points from this day of experiments are entered into an Excel-sheet from which the map in Figure 17 results. The green data points represent burrows that were grouted on the 7th of October 2021 and were already excavated on the 9th of October 2021. Unfortunately, no other data is saved from that day of excavations.

The dark blue data points were also filled with grout on the 7th of October but were not yet excavated, the light blue data points represent the burrow holes that showed smoke during the smoke experiments.

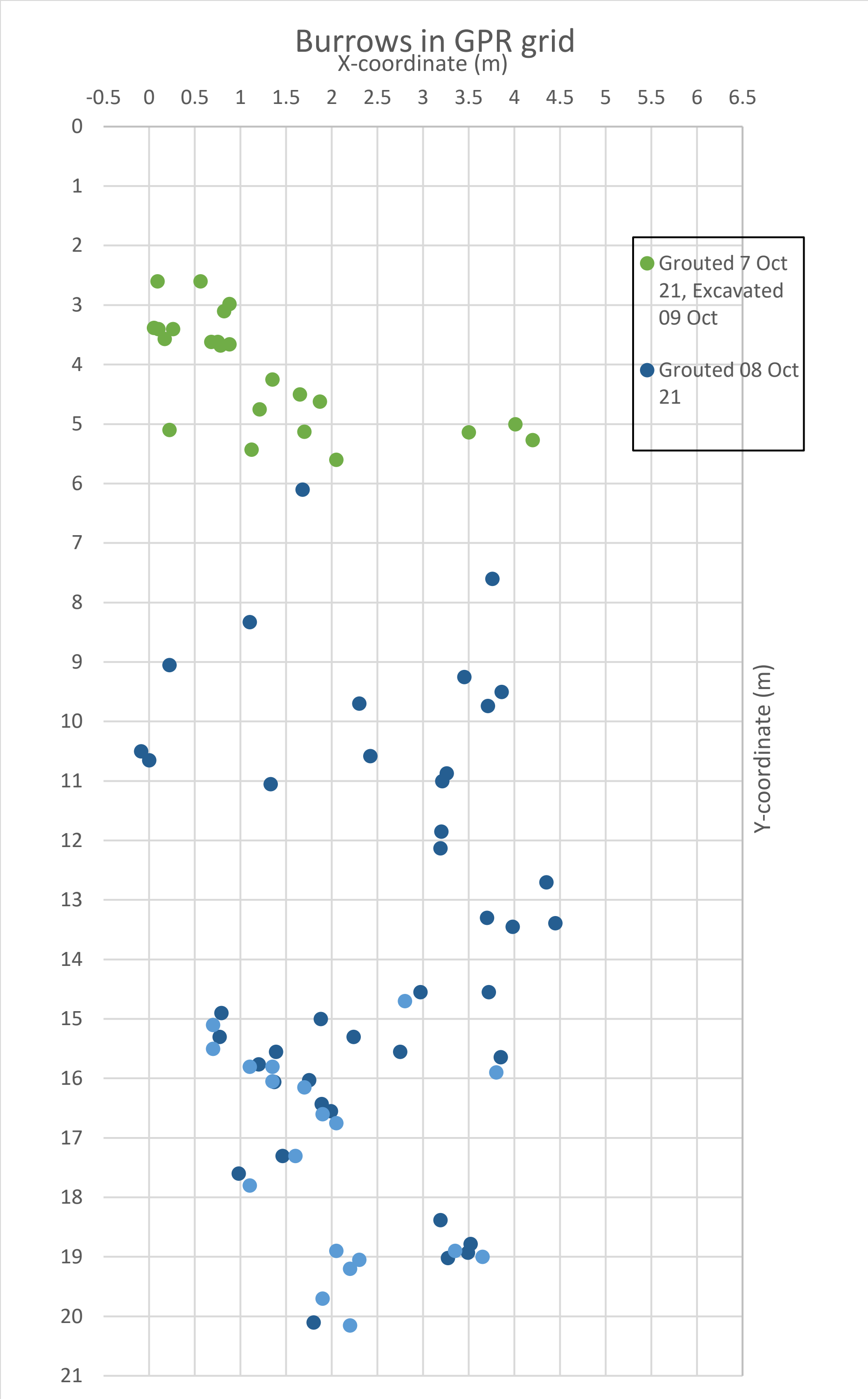

Figure 17: Results from grouting and smoke experiments

During the smoke experiments, the smoke was blown into one hole, which is marked with a red box in figure 18. The other light blue dots indicates the locations of burrow holes that showed smoke and must therefore be connected to the 'start' burrow hole and to each other. It can therefore be concluded that a large burrow system is present here. The smoke experiments also indicated some 'new' burrow holes that originally were not found during the manual inspection of the levee stretch, marked with the black box in figure 18.

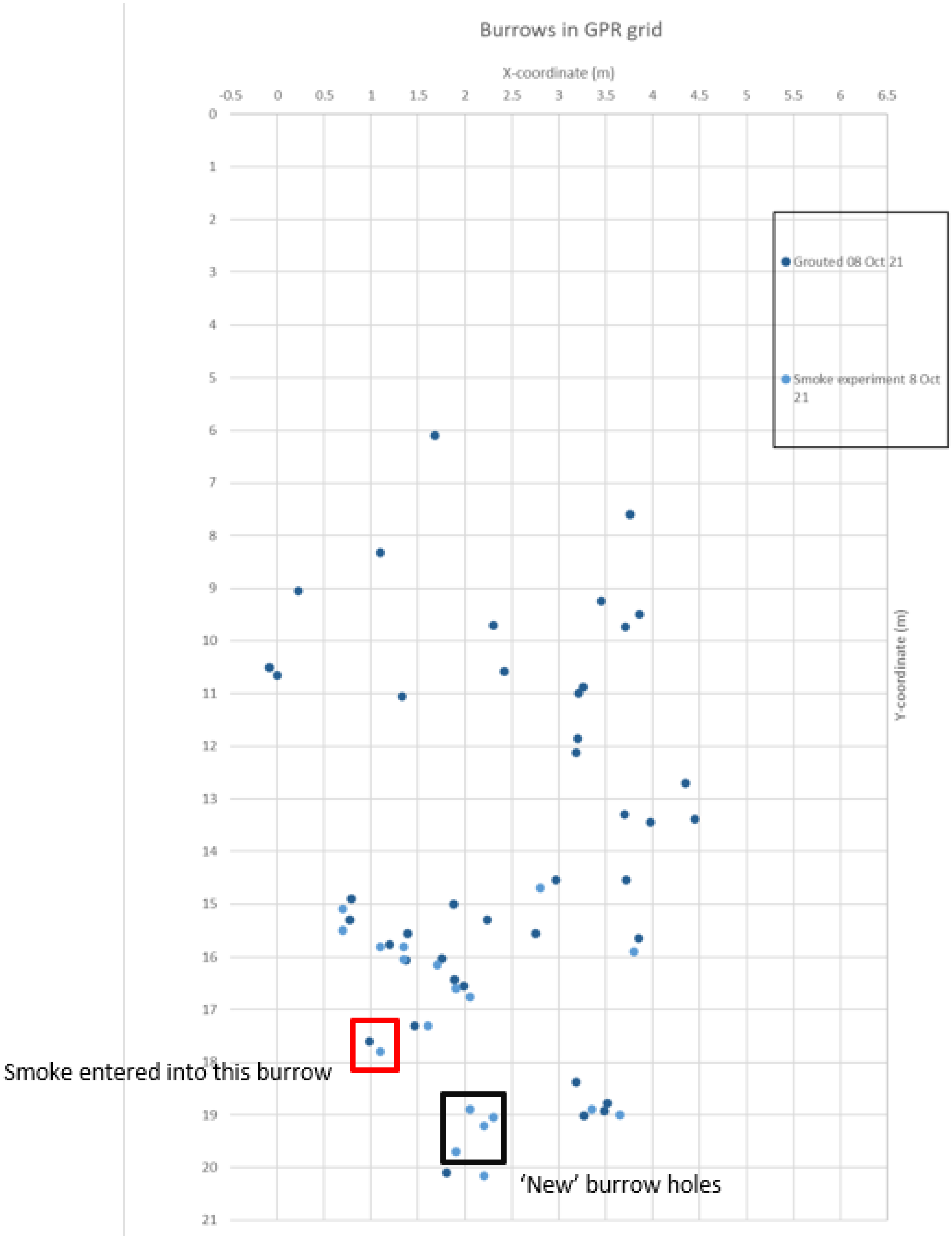

Figure 18: Location of smoke-filled burrow hole and newly found burrows from smoke experiment

At first glance, 13 out of the 19 burrows that showed smoke can easily be linked to the burrows that were grouted, even though a small discrepancy of <10 centimetres can be found which is due to the fact that the locations are manually measured and mapped using tape measures. In figure 18, some of the light blue burrow holes do not overlap the dark blue burrow holes while in reality they represent the same burrow hole. This shows the inaccuracies in mapping and collecting the data during the experiments, chapter 7 recommends a procedure that should prevent this from happening in future experiments.

It can be concluded that smoke experiments are a good alternative to quickly get an indication of the size of the burrow system. The main advantage is the fact that immediate results can be achieved, and immediately conclusions regarding the species that created the burrow can be drawn.

5.1.2 RTK-GPS data from excavations (8th and 9th of February 2022)

The RTK-GPS data can serve as a reference to compare the accuracy of the detection method and to align and link the different data sets. Furthermore, it is useful to map which part of the burrow system was excavated during February 8th and 9th 2022 and where the LiDAR scans were made. Therefore, these RTK locations are also added to the map of Figure 17 and into the LiDAR scans. The LiDAR scans are treated in chapter 5.1.4.

In order to add the RTK-GPS data onto a similar map as for the grouting/smoke experiments, so that the accuracy of the measurements can be assessed, the RD-coordinates from the RTK have to be transformed into the local coordinate system as used during the experiments.

First of all, the coordinate system of the RD-measurements are defined as illustrated in Figure 19 from (kadaster.nl, 2022). Here it can be seen that the values for the x-coordinates for the Netherlands range from 0 in the East till 300 kilometers in the West and the values for the y-coordinates range from approximately 300 km in Limburg to around 600 km in Friesland.

Usually, these coordinates are expressed in meters, as is the case for the RTK-GPS data from the excavations.

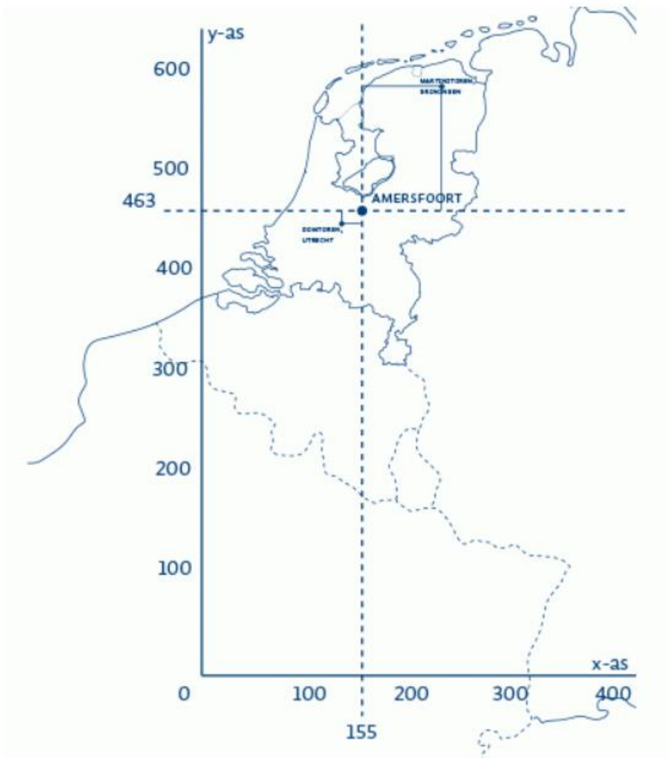

Figure 19: Rijksdriehoeksstelsel coordinate system. Source: (kadaster.nl, 2022)

The orientation of the axes that are used during the grouting/smoke experiments are as follows: the x-coordinates are parallel with the levee crest, and the y-axis runs parallel to the slope of the levee (from the crest down to the toe), which means that the RD-coordinate system has to be rotated with a certain angle. Using an online map, which projects the Netherlands with the same orientation as used for RD-coordinates, the angle between the levee crest and the x-axis used in RD (the 0-180 degree axis on the protector in figure 20) is measured to be 45.6 degrees (Google Maps, 2022).

Figure 20: Angle between RD coordinate system and local coordinate system. Source: (Google Maps, 2022)

This means that the RD coordinate system needs to be rotated with an angle of 45.6 degrees in clockwise direction to have the same orientation as the local coordinate system. Using trigonometric relations, the local coordinates (x' and y') follow from the RD-coordinates (x and y) as described by these formula's (DoubleRoot, 2022).

$$x' = x\cos(\theta) + y\sin(\theta)$$

$$y' = -x\sin(\theta) + y\cos(\theta)$$

Note that the angle θ is defined as the rotation in counter clockwise direction, so in our case, θ=-45.6̊ has to be entered, as illustrated in figure 21 (DoubleRoot, 2022).

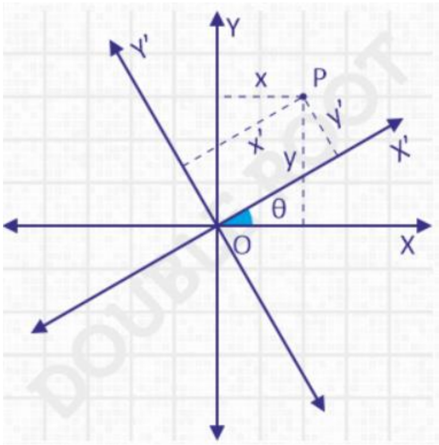

Figure 21: Rotation of axes, source: (DoubleRoot, 2022)

Next up, the y-coordinate needs to be adjusted so that the orientation of the 'top view' which is used in the map, is projected correctly. In other words, where the RTK coordinates represent the location when viewing the levee slope from straight above (vertically), the map projects the location with an orientation perpendicular to the levee slope. This results in a slight change of the local y'-coordinate, which relates to the levee slope as illustrated by figure 22.

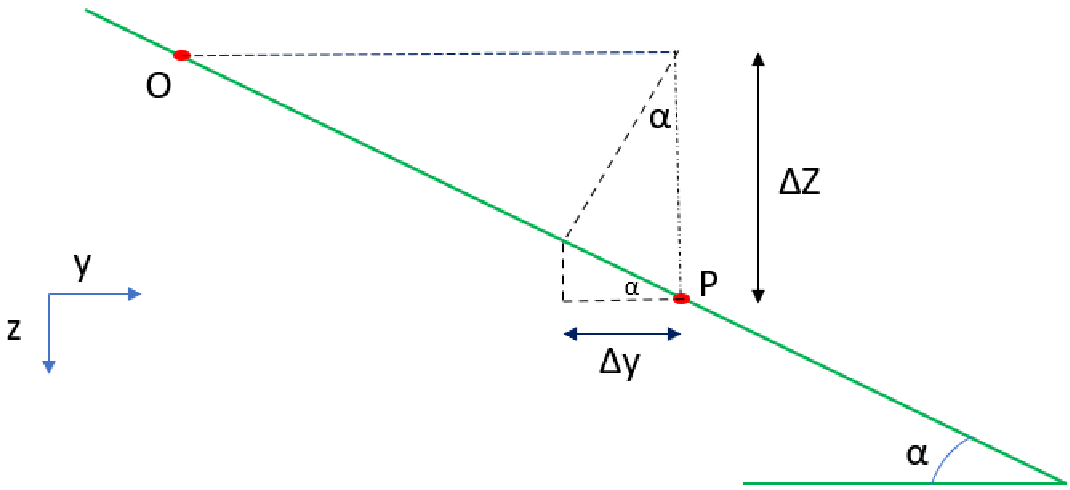

Figure 22: Illustration of the shift in y-coordinate to transform the RTK data into the local coordinate system.

Using a certain pre-defined point at the top of the levee slope as the origin, this shift in y direction, indicated as Δy in figure 9, can be calculated as follows: $\Delta y = \Delta z * \sin(\alpha) * \cos(\alpha)$, where Δz is the difference in z-coordinate between this origin and the point of interest and α is the levee slope angle.

The slope angle of the levee is found using the height data from AHN.nl, which maps the elevation of the Netherlands. Since the actual location of the experiments in in Belgian territory, the data from the same levee but a couple of tens of meters in Dutch territory is used. A cross section of the levee elevation is made from which the slope is estimated to be (3H:1V), as the vertical deviation is 7 meters over a horizontal distance of approximately 20 metres, illustrated by figure 23 (AHN.nl, 2022).

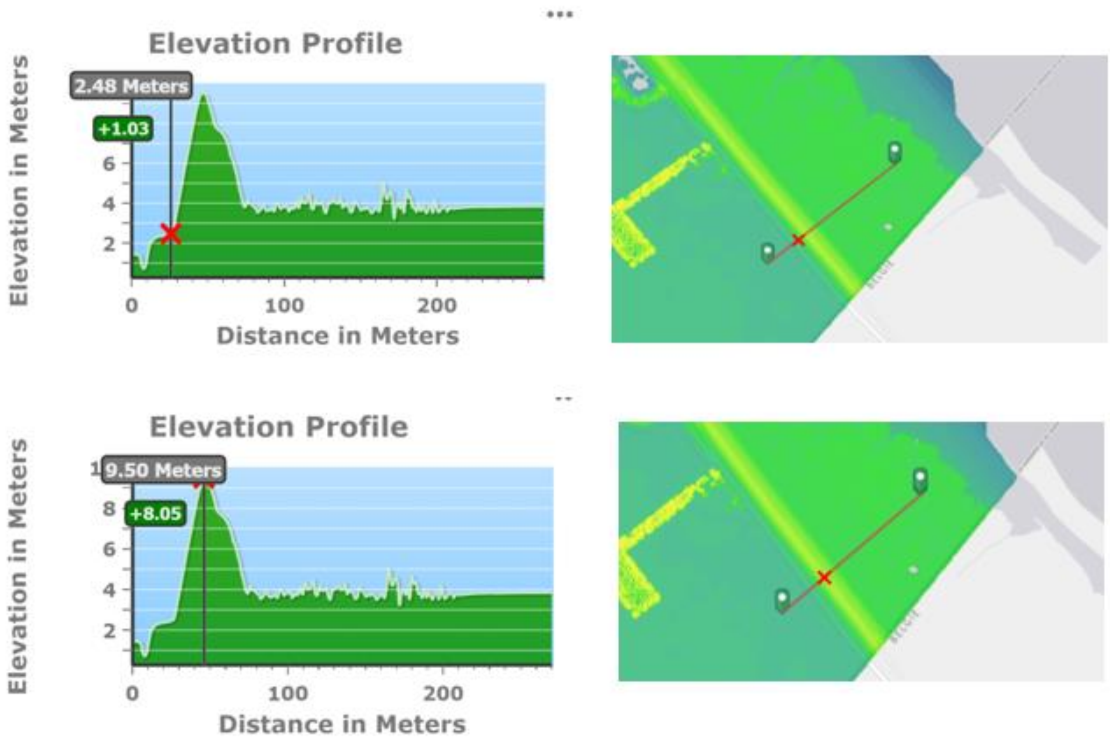

Figure 23: Retrieval of the levee slope angle using cross sections from AHN.nl Source: (AHN.nl, 2022)

In Figure 23, the top left and bottom left images show the location of the measurements in the cross section and corresponding heights, and the images on the right show the top view location of these measurement points.
Applying these transformation to the RTK data, leads to Figure 24, showing all the RTK-data points that are collected on February 8th and February 9th 2022. The yellow dots show the data points that are collected on 08-02, and mainly represent burrow entrance holes. The green dots represent characteristics points from the excavation of these burrow system, many of which have also been scanned using the LiDAR.

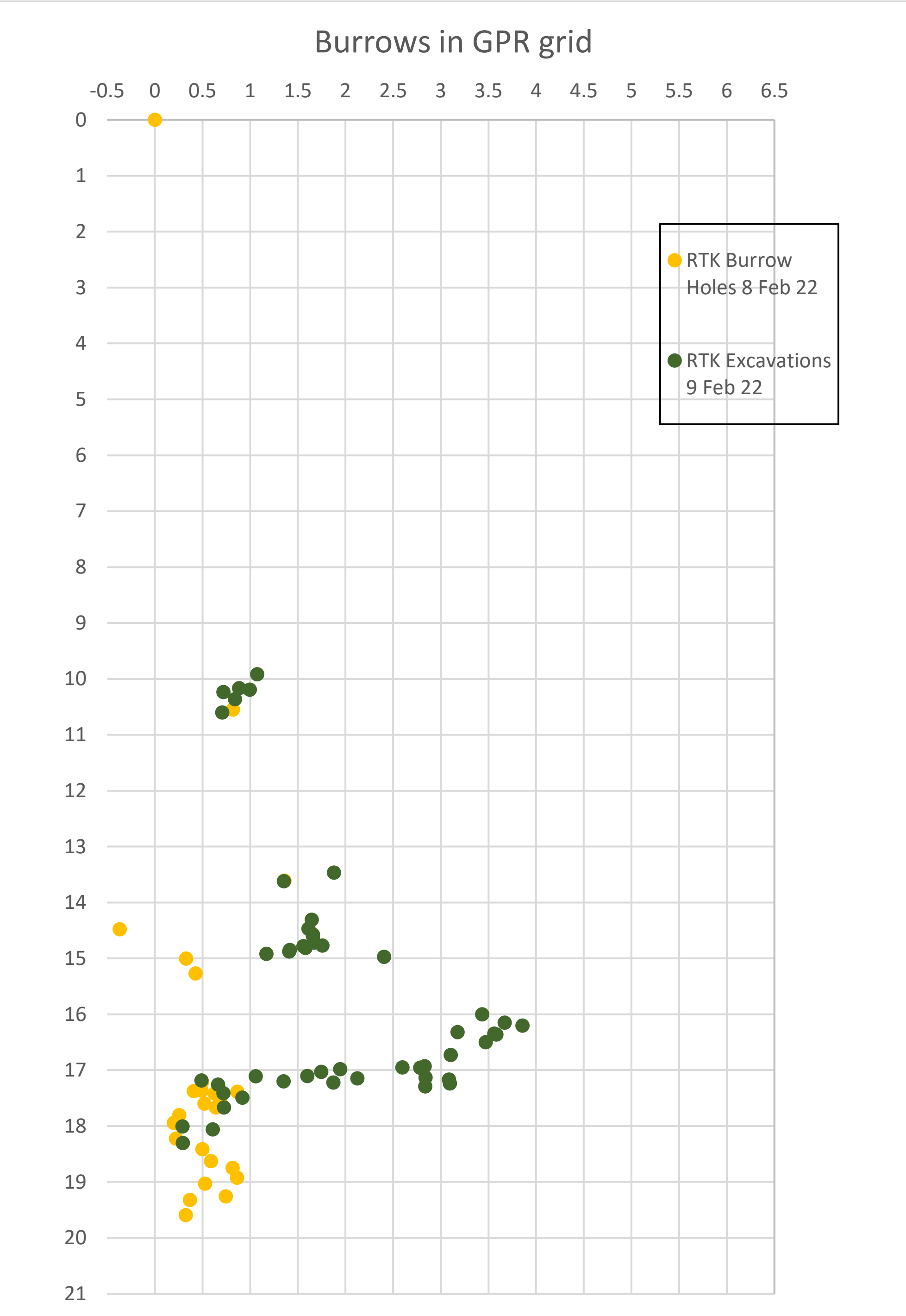

Figure 24: Mapping of the RTK coordinates on the local coordinate system

These data points can now be combined with the grouting and smoke experiment data points from Figure 17. However, this would rely on the assumption that the origin is the same in both maps. While it is known that in both cases a point 'on the landside edge of the asphalt road' on the levee crest is used, there is no exact record that in both instances the exact same origin point is adopted. Thus, it has to be noted that in reality the x-coordinates of the RTK data points could be shifted a couple centimetres, but assuming a nearly identical origin point, the data from the two experiments can be combined into figure 25.

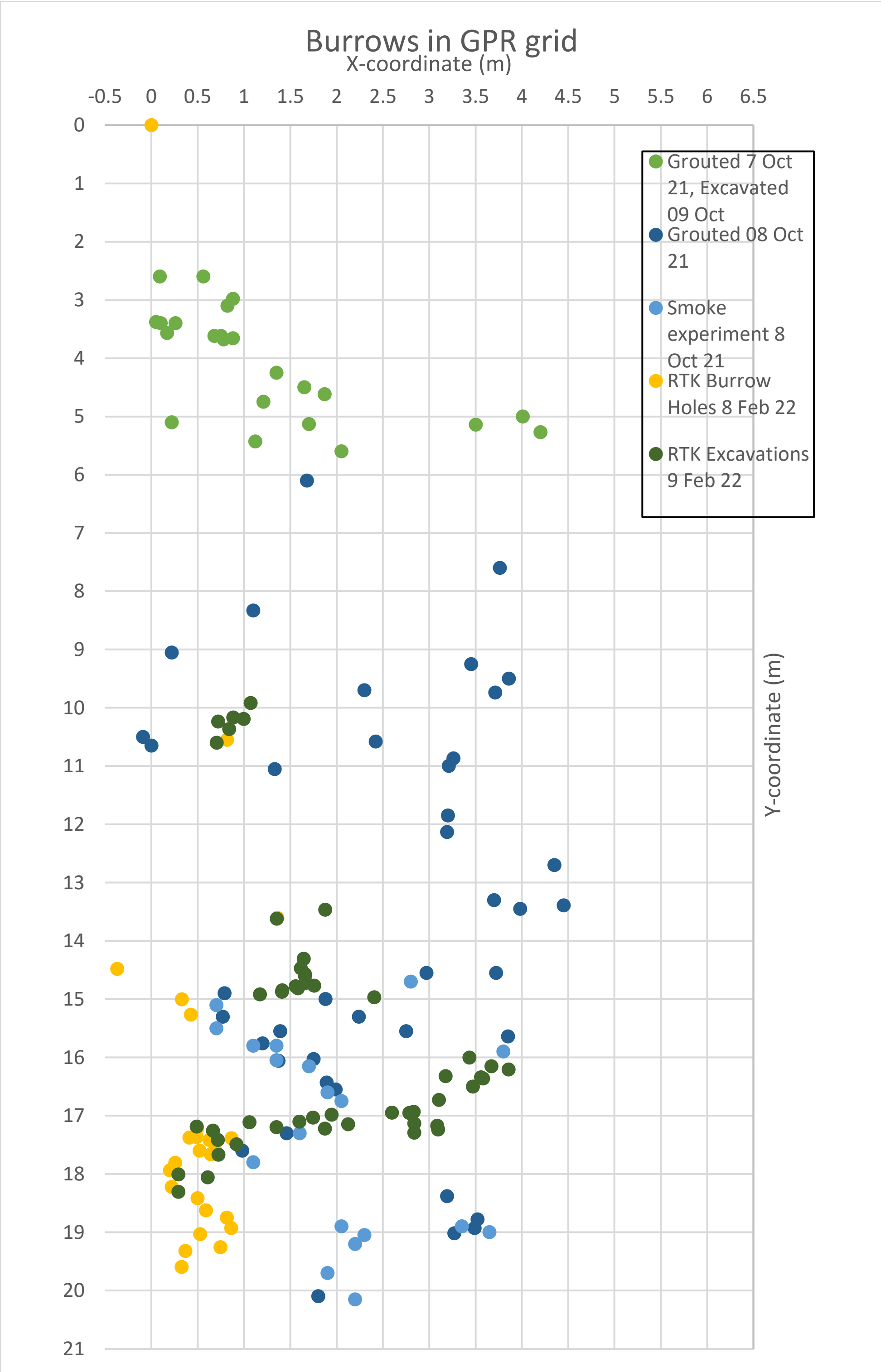

Figure 25: Combining the RTK data points with the grouting and smoke experiment data

5.1.3 GPR data

In order to be able to assess the accuracy of the different type of detection methods, it is important that these methods have been used on the same stretch of the levee, otherwise there is no reference to compare each of the results to. Since we now know the locations of the grouting, smoke and excavation experiments, the next step is to identify the areas that have been scanned by the GPR. Figure 26 shows these areas as labelled Z1 and Z2 compared with the full data map.

Figure 26: GPR scanned zones combined with the full data map

Figure 27 shows only the excavated data points in comparison to the GPR zones

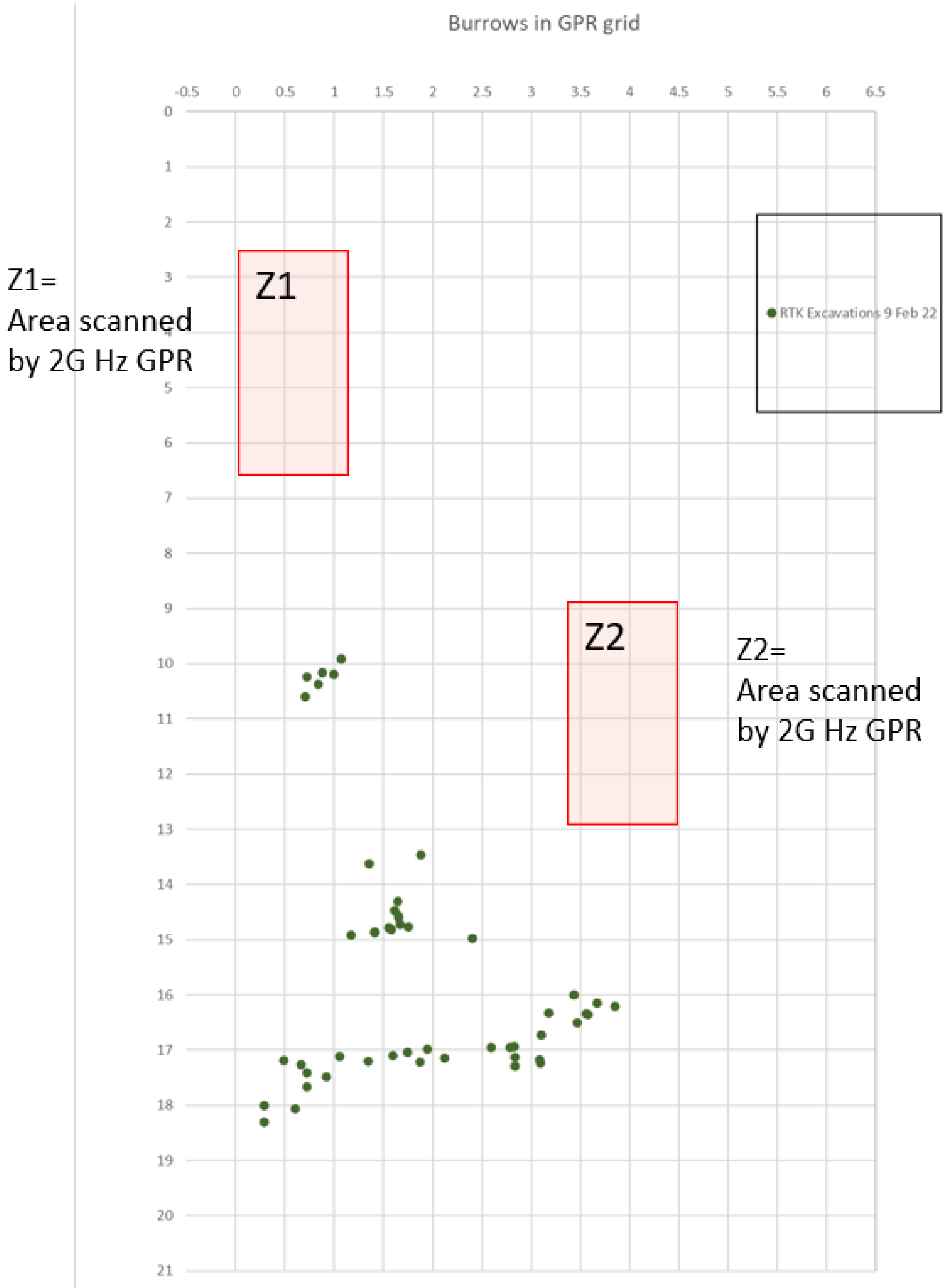

Figure 27: GPR scanned zones combined with the RTK locations for the excavations

It can be concluded that there is no area that is both scanned with GPR and excavated, which makes the interpretation and assessment of the GPR data almost impossible.

5.1.4 LiDAR scans

Several LiDAR scans have been made on the 9th of February and the software CloudCompare is used to process these scans. Figure 28 shows the full excavations that have been carried out that day with the RTK data points added on top. The RTK coordinates are aligned to the LiDAR scans by taking 3 datapoints from which the location is most accurately known from pictures taken during the excavation on Feb 9th and using the registration tool called 'Align (point pairs picking)'. For this procedure, the points labelled Robert 1, Robert 2 and Robert 9 were used as they were most easily recognisable on the LiDAR scan.

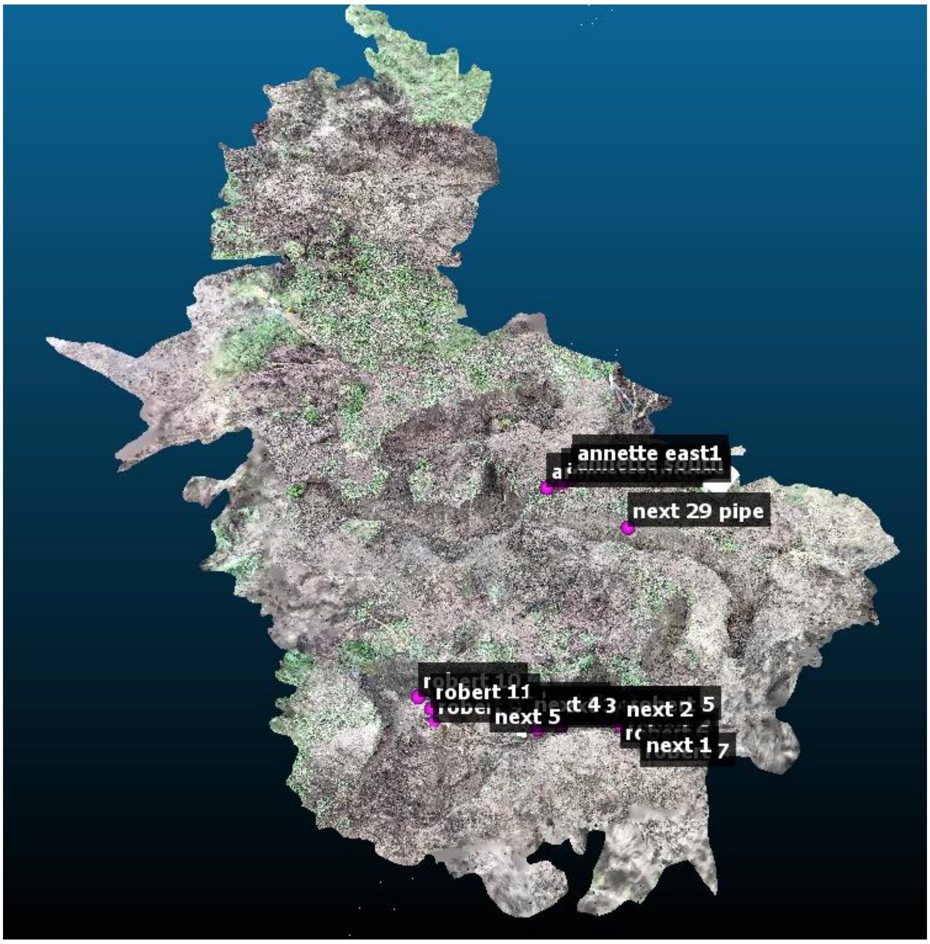

Figure 28: LiDAR scan of the full excavated area

The grouted burrow system is best visible in the stretch of data points which are labelled 'Robert 1' till 'Robert 11', as shown in figure 29.

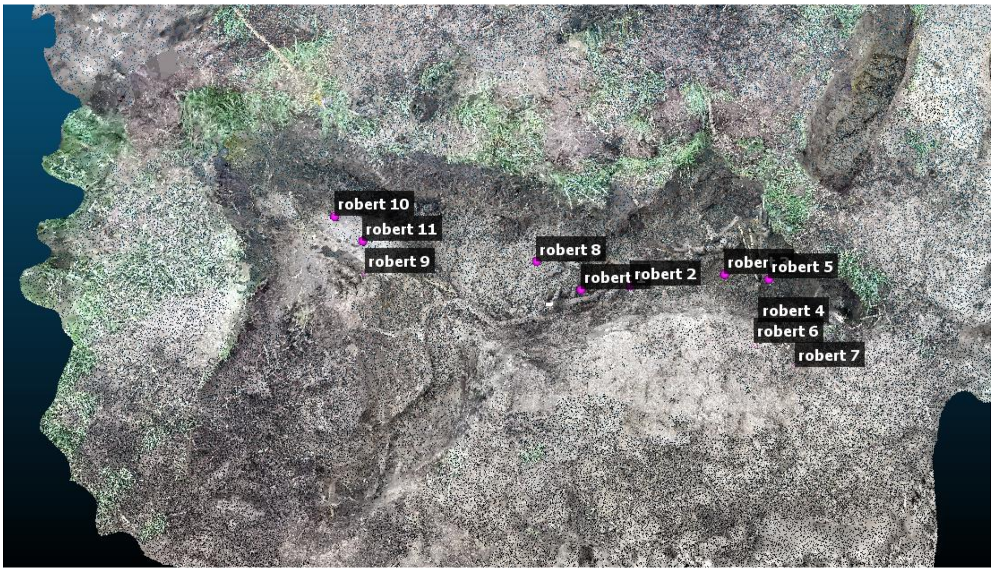

Figure 29: LiDAR scan of most detailed stretch of excavated burrow

The area that is LiDAR scanned can now also be added to the total map showing all the data, resulting in Figure 30.

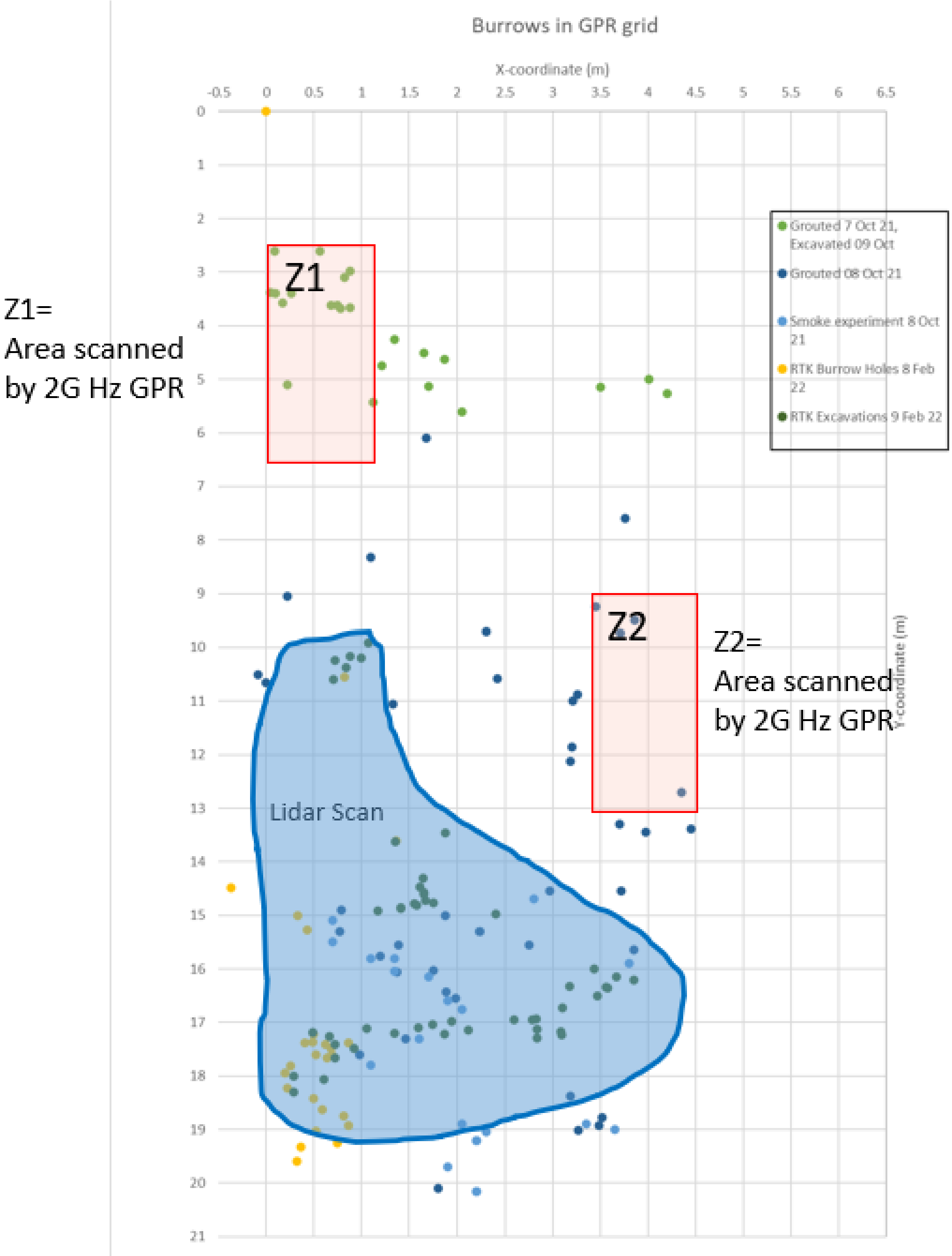

Figure 30: Full map of all data points, highlighting the areas scanned by GPR in red and LiDAR in blue.

5.2 Data analysis

This chapter aims to distribute the found burrow holes from the grouting and smoke experiment into burrow groups/systems, using the conclusions from chapter 3.2 in combination with the excavated burrow tunnels during the experiments on February 9th 2022 to make assumptions regarding the responsible burrowing species. Afterwards, the spatial distribution of the burrow holes within these groups are further analyzed, especially the burrow density per m^2 which is relevant for the probabilistic model in chapter 6.

5.2.1 Burrow system identification

First of all, during the grouting experiments, for a number of holes the amount of grout that was poured into it was recorded. This can be used to estimate the total length of the underground tunnels by assuming a mean tunnel diameter of 3 centimeters, which is validated by the recorded burrow hole diameters from grouting experiments on the October 7th, see appendix A.

The total tunnel length that stems from these burrow holes can be used to connect it with other burrow holes. Figure 31 shows from which holes the amount of grout is known and the corresponding amount of grout in liters.

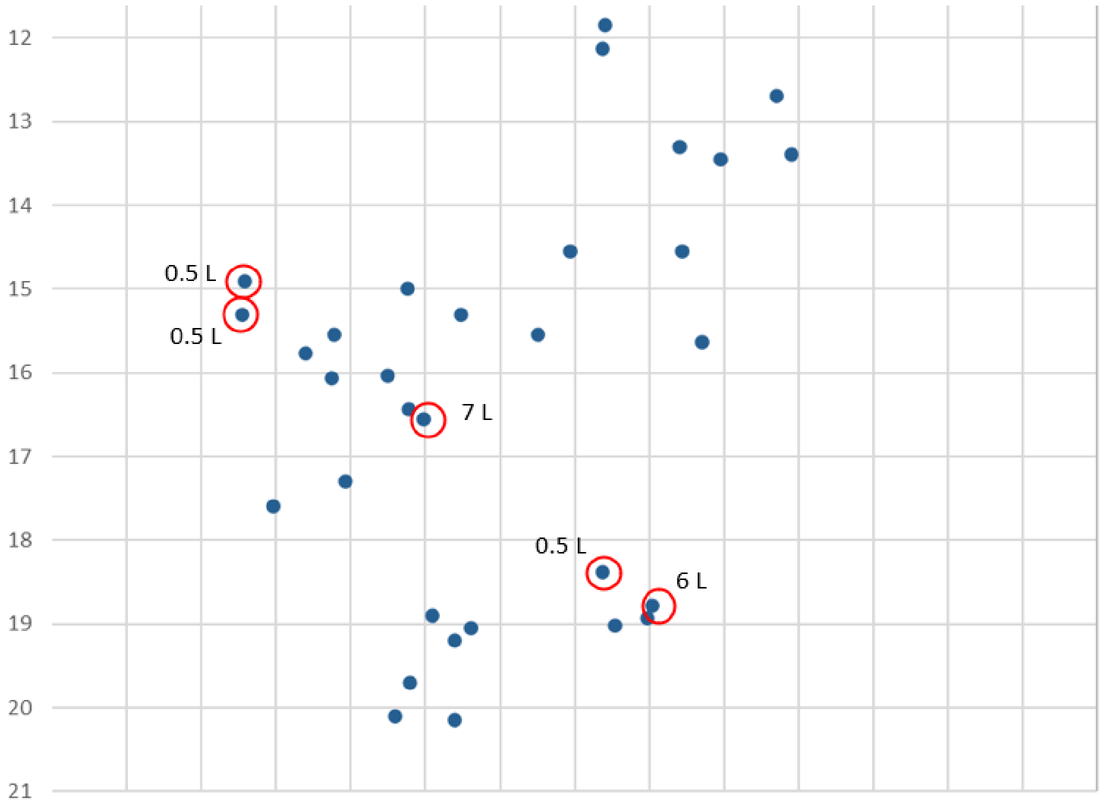

Figure 31: Amount of grout poured into burrow holes

Assuming the burrow diameter of 3 centimeters, a circular cross section and thus a cross sectional area of 7.07 cm^2 leads to a tunnel length of 9.9 meters for an amount of 7 liters, approximately 8.5 meters for an amount of 6 liters and 0.7 meters for an amount of 0.5 liters. From this is can directly be concluded that a total tunnel length of almost 10 meters, from the hole that took 7 liters of grout, is relatively long and probably too long to be part of a vole burrow system. Especially regarding the fact that this hole seems to part of a larger group of burrows above it.

It is now interesting to predict which burrow holes can be connected to each grout taking burrow holes based on the calculated total burrow length. For this, the distance between the grouted burrows and the nearest separate group of burrows is necessary, visible in figure 32.

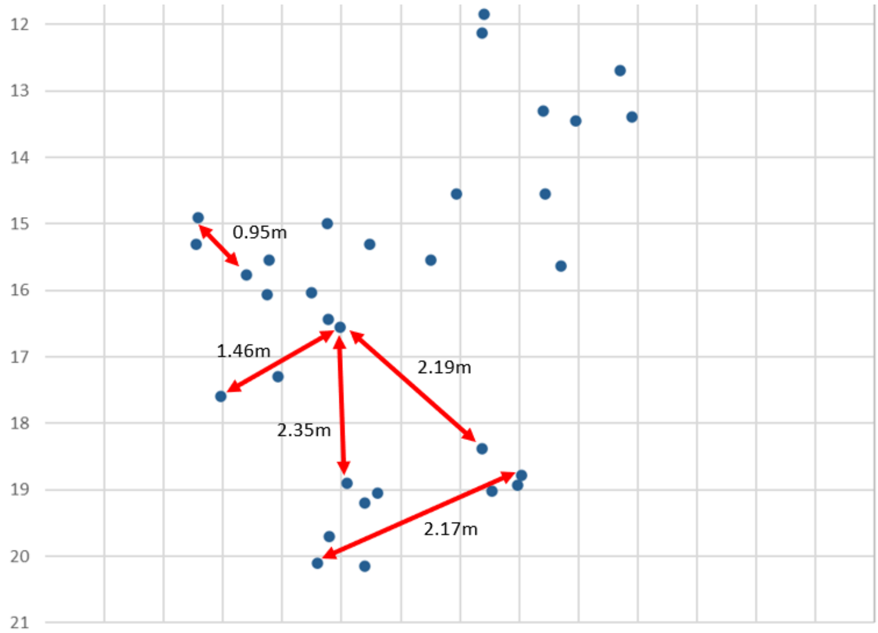

Figure 32: Distance between burrow groups.

In practice, tunnels will not be perfectly linear and branches are known to occur. This is also known to be the case from the excavations on February 9th which occurred in the vicinity of these burrow groups. Appendix B shows additional images, where the excavated tunnels are visible. On an excavated tunnel of approximately 2.5 meters, four junction have been found consisting of 2 branches each. This frequency of branching should also be taken into account when trying to recreate the assumed tunnels. Furthermore, combining Figure 31 and Figure 32, it can be concluded that the grouted burrow holes take enough grout to be connected to each of the nearby burrow groups, further hinting towards the fact this burrow system is constructed by a mole, as the total tunnel length and burrow area would far exceed the typical values for vole burrows. Figure 33 shows an example of how the different burrow groups can be connected based on the amount of grout poured into the burrows and the tendency of branches to be present. While it is unknown if this is actually how the tunnels run in this stretch of the levee, since there are no excavations here to validate it, it does show that the different burrow groups can easily be connected and belong to the same system created by the same mole.

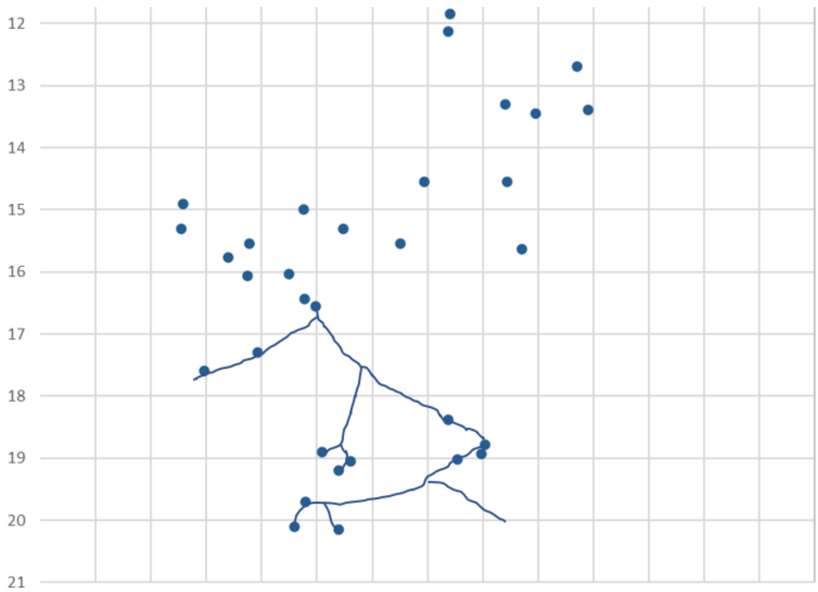

Figure 33: Example of how burrow groups can be connected to the same mole burrow system.

The remaining burrow holes will be investigated next. Higher up the levee slope, around y = 3 meters and x= 0.5 meters, so roughly the area that is marked as Z1 in Figure 30, a remarkable high burrow hole density is found and multiple burrow holes are almost right next to each other. This could hint towards 2 vole nests, one at (x=0.2;y=3.5) and one at (x=0.7;y=3.6). As we know these usually are located at the center of the vole burrow system. It is not uncommon for vole burrows to have multiple nests, the beforementioned research has recorded vole systems with up to 3 nests interconnected by tunnels (Brügger, Nentwig, & Airoldi, 2010).
The location of this vole burrow system was part of the excavations on October 9th 2021 from which no records were made, we can therefore not validate this assumption. However, during the excavations on February 9th, a small burrow system which has the characteristics of a vole burrow system and was identified as one at the time, see figure 16, was found somewhere near this location. While no exact coordinates were measured of this part of the excavations, it is very possible that this was indeed one of vole burrow systems that we can recognize from the map, possibly the excavations from October 8th 2021 were covered with soil again and this vole burrow system was dug up the second time around on February 9th 2022. Whether this theory is true or not is hard to validate but it doesn't influence the fact that there is a vole burrow system assumed to be present in the top left part of this levee stretch, as visible in Figure 34.

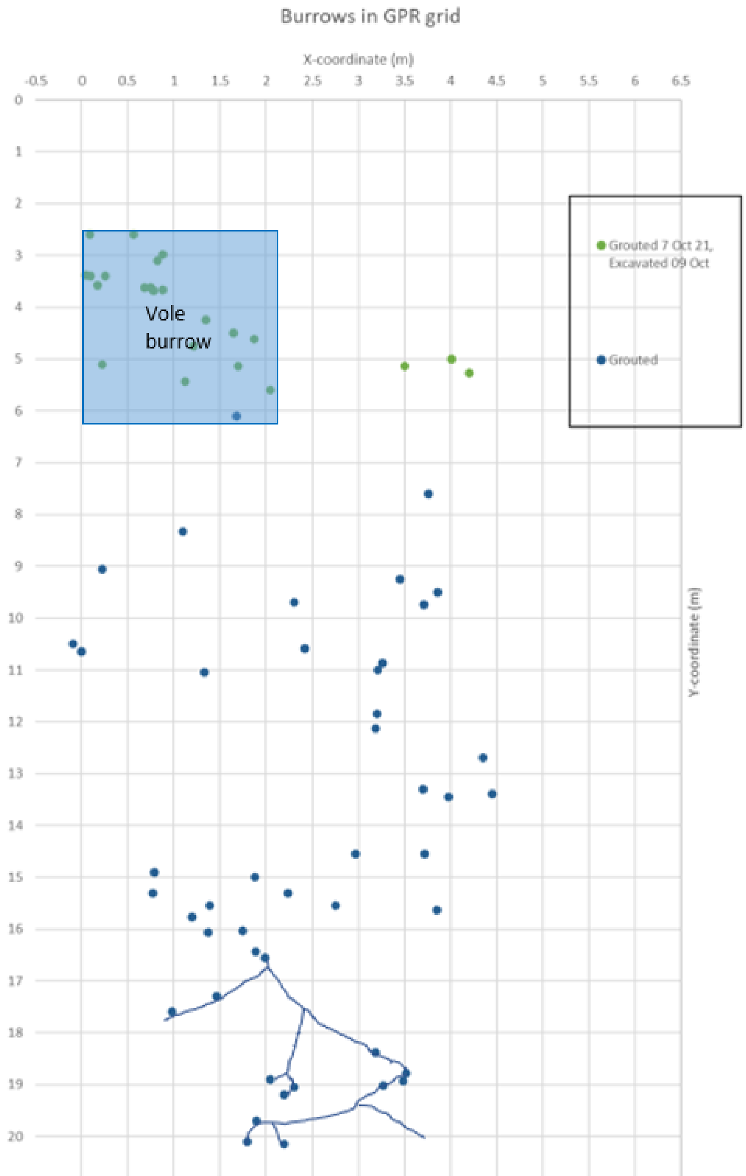

Figure 34: Location and size of vole burrow

For the group of burrow holes that stretches from right above the drawn tunnels towards the right of the levee stretch, we can use the excavations on February 9th, also visible in Figure 14 and 15, to prove it to be part of a mole burrow system as it coincides with the excavated area which is also LiDAR scanned. The length of the tunnels is simply too long to be part of a vole burrow system. Appendix B can again be used for additional pictures of the excavations that were done at the location of this burrow group. We can conclude that the mole burrow system further expands up the levee slope, figure 35 below shows how the LiDAR scanned area, and thus the locations of the excavations, relates to the burrow holes.

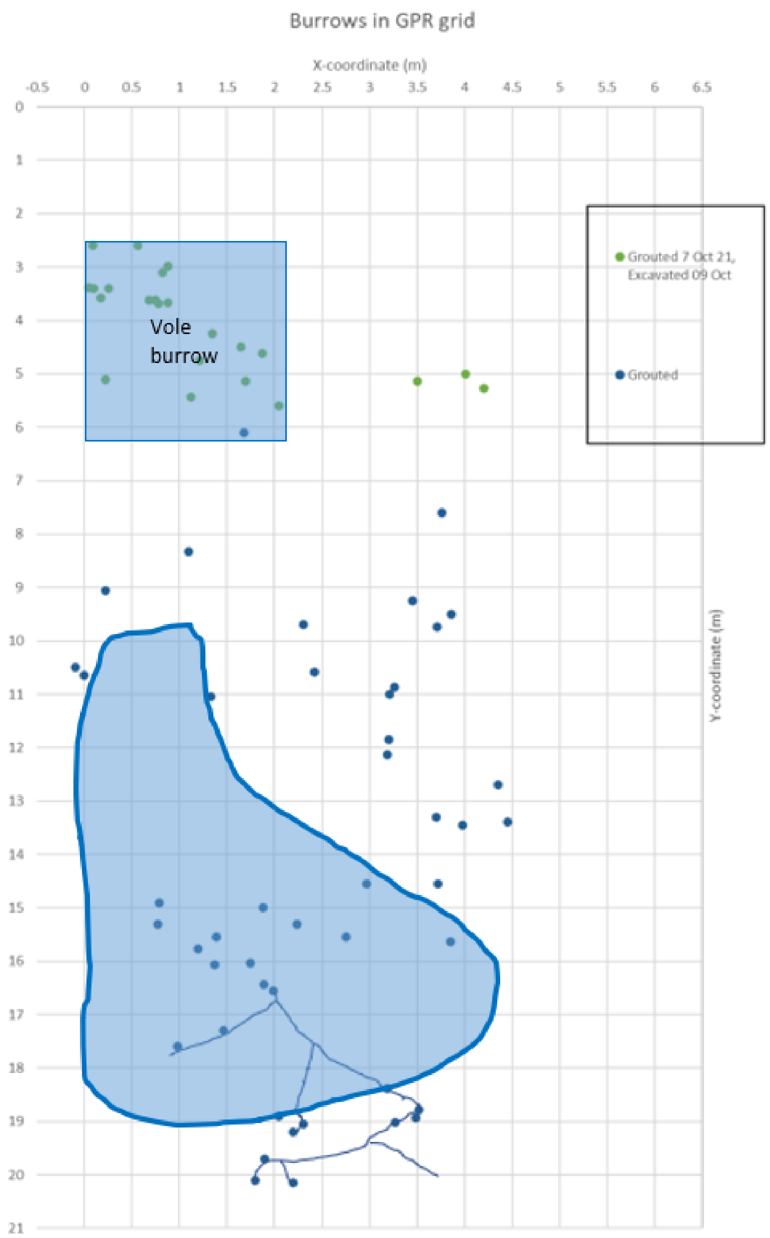

Figure 35: Location of LiDAR scanned area, where mole tunnels were excavated

In fact, it is probable that besides from the vole burrow system, all the other burrow holes belong to the same mole burrow system. A reason for this is that no clear vole burrow characteristics can be distinguished from the burrow points as nests cannot be recognized. The only other option would be multiple separate mole burrow systems in this stretch. However, considering the behavior of moles, this is highly unlikely. Moles are known to be solitary animals who are highly protective of their own habitat. In fact, moles are known to fight each other in the rare case were two mole system intersect each other and they will only leave their system when it's mating season (Mellanby, 1971). In previous research at a nearby levee stretch, linear patterns could easily be recognized in a mole burrow system. While this is less obvious here, a certain 'pathway' of the mole burrow tunnel can still be identified, as visible in Figure 36.

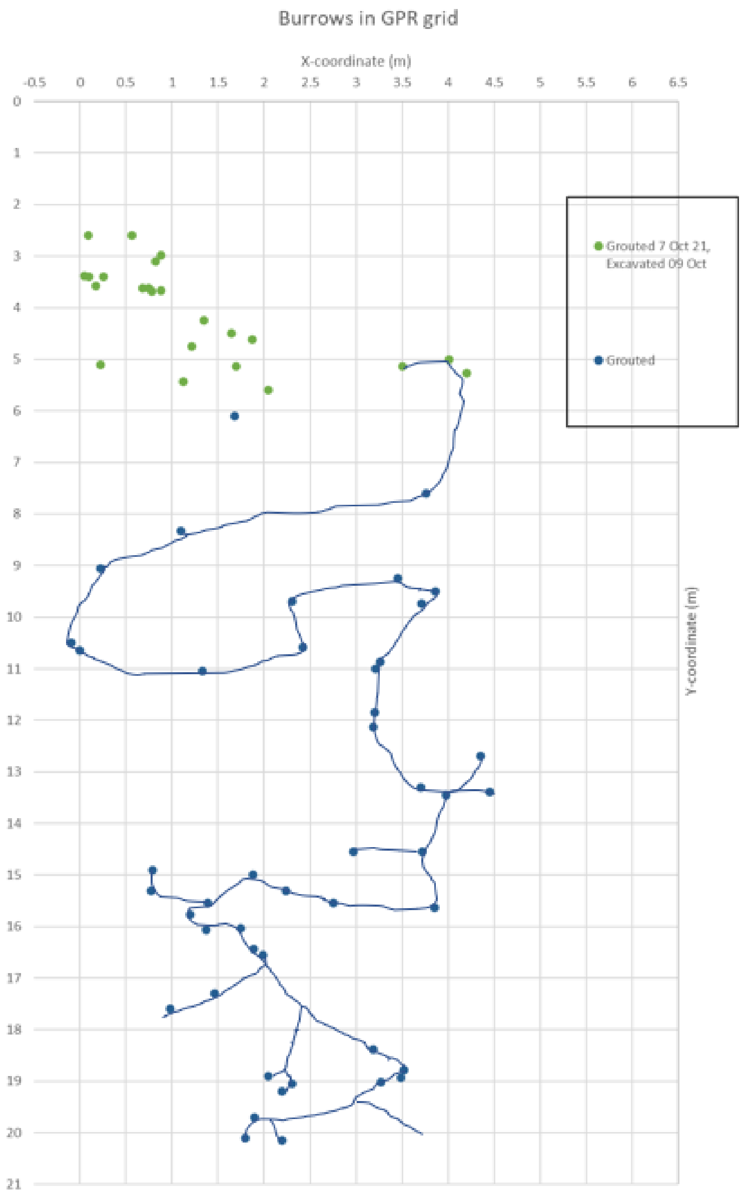

Figure 36: Pattern visible through mole burrow holes, line shows possible trajectory of mole tunnel through the levee

Combining this with the characteristic size of mole burrow season can pretty much confirm that the remaining burrow holes are all part of the same mole burrow system. Figure 38 shows the areas of the two burrow system that can be distinguished on this levee stretch.
We can now start to look at the geometrical characteristics of these systems.

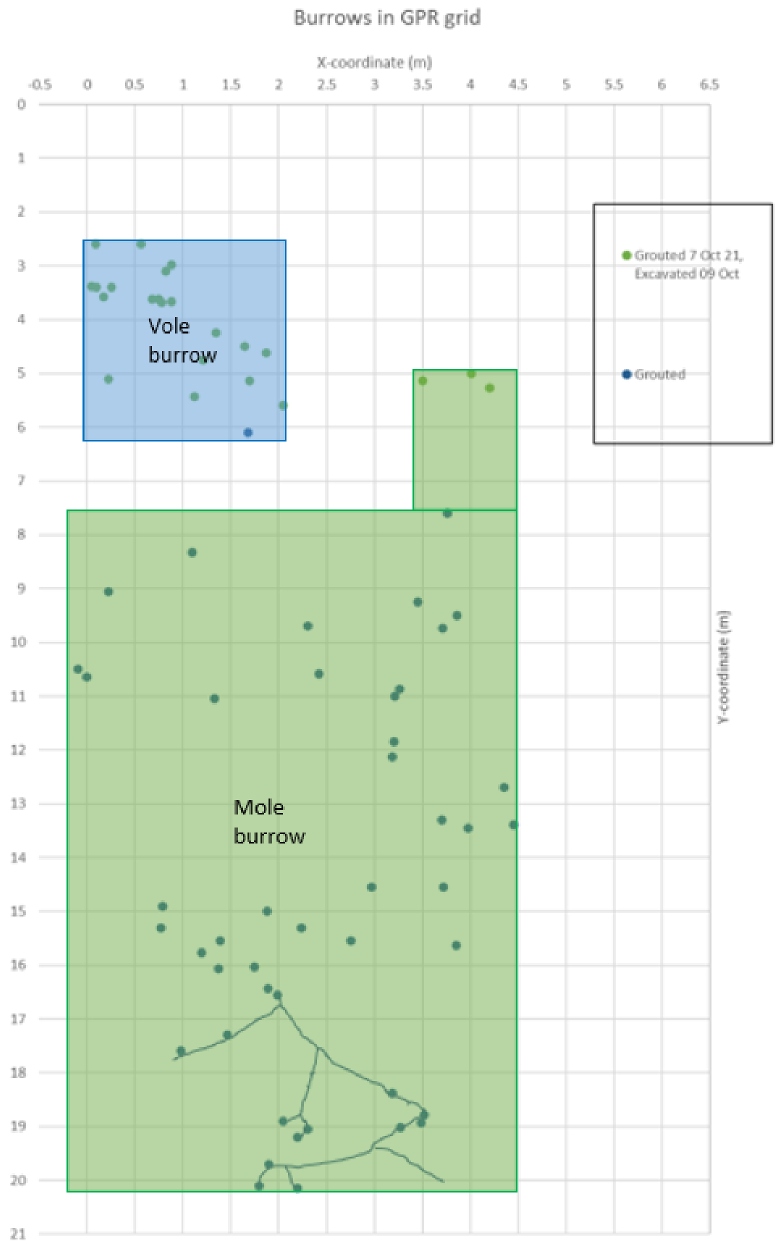

Figure 37: The size and location of identified burrow systems

5.2.2 Burrow system analysis

The first parameter that needs to be investigated is the burrow hole density, so how many burrow holes can we expect to find for vole and mole burrow systems per m^2 based on the information we have. We first need the burrow area, which is shown in figure 38. The area for the vole burrow is found to be 8 m^2, which is in the range that we found in chapter 3. The total area for the mole burrow is approximately 64 m^2, which is small for a mole burrow system but it has to be noted here that this probably is not the complete mole burrow system, as only the part of the system that lies within the 4 meter wide levee stretch is counted. This should however not affect the found burrow hole density too much, assuming the remaining undiscovered part of the mole burrow will show the same characteristics.

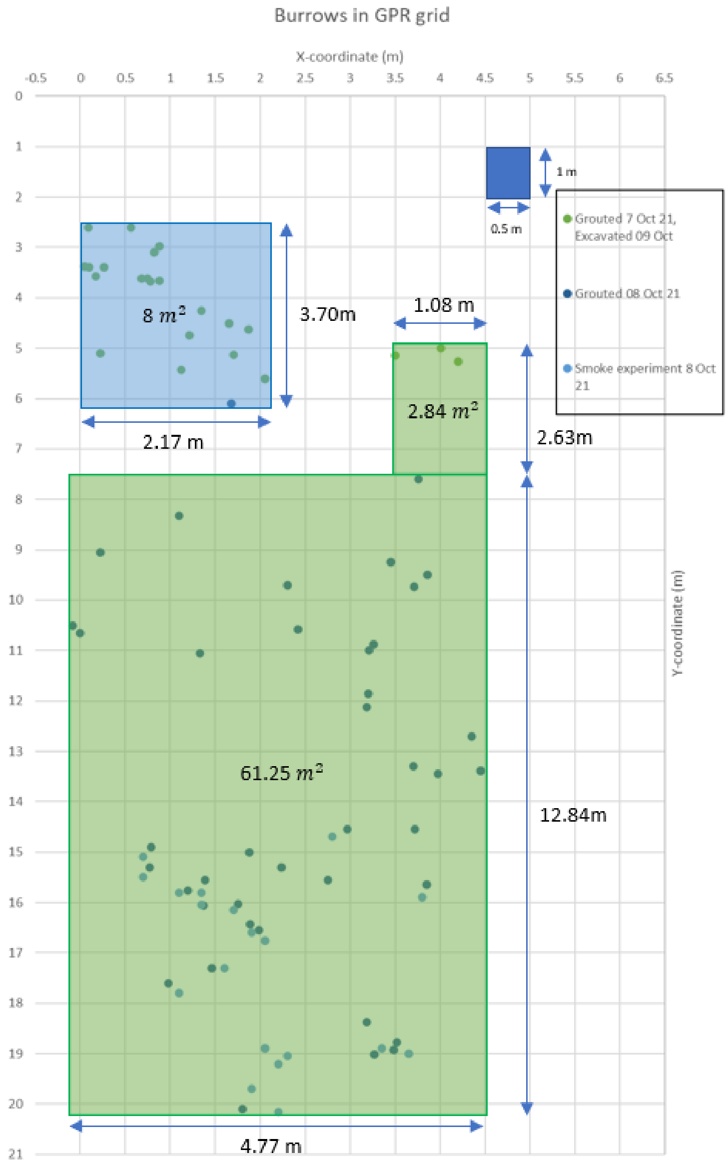

Figure 38: Burrow group surface area

For the calculation of the surface area, rectangles are fitted that enclose the shortest area around the burrow group. This is done for simplicity, since the scale on the y- and x-axis is different. In case more accurate results are wished, one could also choose to fit a polygon, however the difference in outcome is deemed to be negligible and exceed the purpose of this analysis.

The vole burrow contains 21 burrow holes, resulting in a burrow hole density of 2.6 burrow holes per m^2. The mole system contains 47 burrow holes, resulting in a burrow hole density of 0.7 burrow holes per m^2. This information will be used in the probabilistic model in chapter 6 to distinguish vole and mole burrow systems.

Next up, the recorded burrow hole diameter and depth are collected into a histogram, with the aim to examine whether there is a clear difference to be seen between the vole and mole burrow system. Figure 39 shows these histograms.

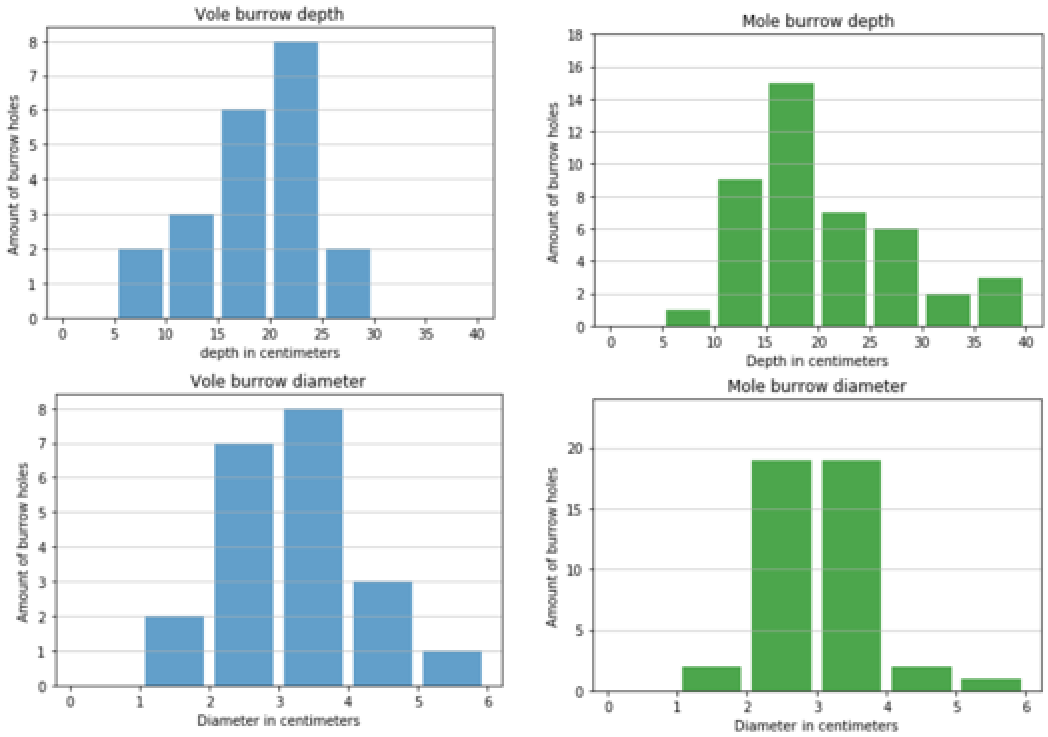

Figure 39: Histograms comparing the distribution of vole vs mole burrow depth and diameter

No clear conclusions can be drawn from these histograms, both vole and mole burrow holes show similar distributions of burrow depth and diameter. Mole burrow depth can reach greater depths than vole burrows, which is expected from literature but in these instances the majority of mole burrow holes are the same depth or even lower than the mode for the vole burrow hole depth. The same can be said for the diameter of the burrow holes and thus we can conclude that no distinction between vole and mole burrow holes can be made based on their burrow hole depth and burrow hole diameter and therefore this parameter should not be taken into account when developing the probabilistic model in chapter 6.

One of the main goals of the model should be to give an estimation of the expected number of burrow holes within a certain area, based on whether this burrow group is identified as a vole or mole burrow. The exact way in which the model will do so is described in Chapter 6 but a crucial parameter is the distance from a burrow hole to the nearest burrow hole. More specifically, the model should generate realistic values for this parameter based on the experiment data, the way this is achieved is by fitting a realistic probability density function through the data.

Firstly however, Figure 39 shows the histograms that belong to the distribution of the distance from each burrow to the nearest burrow. The value for this distance is retrieved by computing the linear distance from each burrow hole to every other burrow hole in the group and taking the smallest value. The python script for this step can be found in Appendix C. Figure 40 shows the histogram for the vole burrow group on the left (in blue) and for the mole burrow group on the right. The mean value for this shortest distance to the nearest burrow hole is given in the plots as well.

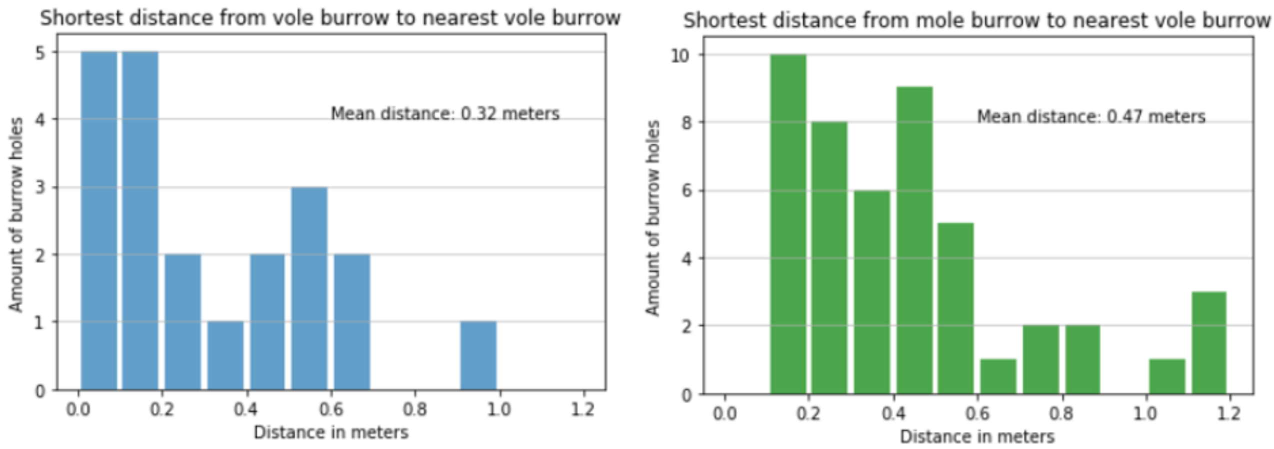

Figure 40: Histograms showing the distribution of the shortest distance from a vole burrow hole (left) and a mole burrow hole (right) to the nearest burrow hole.

In figure 40, the width of each bin is equal to 0.1 meters, the first bin is running from 0 to 0.1 meters, the second one runs form 0.1 meters to 0.2 and so forth to the last bin running from 1.1 to 1.2 meters. As expected, vole burrow are usually closer together while mole burrow can spread out over a larger distance more which is explained by the characteristically longer tunnel length for mole tunnels. Shorter distances seem to be the most frequent in both histograms, with some outliers at larger values. Although none of the distributions that were fitted lead to a good match, due to the small amount of data points, in both cases the distributions are found to best be described by a Gumbel distribution which is commonly used in distributions regarding extreme values (Jonkman, Steenbergen, & Morales-Nápoles, 2017). This decision was made based on visual interpretation of fits with several distributions. Python is used to fit this Gumbel distribution through the data, as visible in Figure 41. The value for the two fitted parameters, the location and the scale, are visible in the title of the two plots.

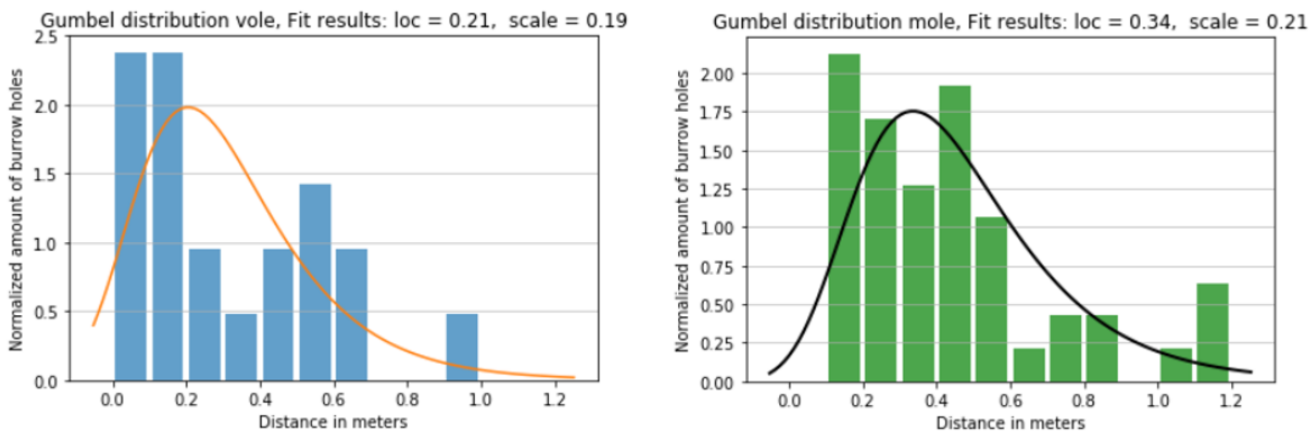

Figure 41: Gumbel probability density function fit through the normalized vole histogram (left) and mole histogram (right)

Figure 41 shows the two normalized histograms, which means that the sum of the areas of the bins add up to 1. This is done by dividing the bin count by the product of the total amount of observations and the bin width. For example, for the mole the first bin counts 10 of the 47 observations, which leads to the normalized amount of burrow holes: $\frac{10}{(47*0.1)} = 2.12$. In this way, the fit of the pdf is better visible. While both pdf's show a decent fit with the data, the small sample size (especially for the vole burrow histogram) lead to some discrepancies in the fit. This can be improved in the future by collecting more data by performing more visual inspection, so that the data volume is increased leading to a smoother pdf fit. For now, this result will be used and applied in the probabilistic model in the next chapter. The main conclusions from this chapter, on which the probabilistic model will partly be based, are:

- Burrow groups with a surface area in the order of 20 m^2 or less can be identified as vole burrow system
- Burrow groups with a burrow hole density of 2 burrow holes per m^2 or more can be identified as a vole burrow system, groups with a density of less than 2 holes per m^2 can be identified as a mole burrow system. This value is achieved by taking the mean value for the distance to the nearest burrow hole from Figure 40, assuming a circular area with this mean value as the radius of the circle and taking the reciprocal to retrieve how many of these circles would fit in 1 m^2. For vole burrows, this density is equal to 3.5 burrow/m^2 and for moles the density is 1.4 holes/m^2. The value of 2 is chosen as a safe boundary as the experiment data showed a vole burrow system with two nests, which is rare, leading to a higher burrow density than expected to be found in practice.
- It can be concluded that the probability density function for the shortest distance from a vole burrow to the nearest vole burrow can be described by a Gumbel(μ=0.21,β=0.19) distribution and the probability density function for the shortest distance from a mole burrow to the nearest mole burrow can be described by a Gumbel(μ=0.34,β=0.21) distribution. Here, the μ is the location parameter and β is the scale parameter.

Chapter 6: Probabilistic model

In this chapter the layout for a probabilistic model is given that aims to facilitate the manual inspection of a levee stretch. It uses the conclusions made in chapter 5, based on the data that is retrieved during the experiments and analyzed accordingly.
The model should predict which animal, a vole or a mole, is responsible for the burrow. Furthermore, it should predict the expected amount of burrow holes within the burrow group area which could be used by the inspector to determine the quality of his investigation. In addition to this, the model should assess the quality of the inspection as well, by returning the probability that there is at least one more burrow hole in the investigated area. If the model would return a large value for this probability, the inspector can conclude that a more thorough search of the area is needed since he or she missed some burrow holes. Missing burrow holes is common in practice, as described by (Tsimopoulou & Koelewijn, 2022), in a report that includes the manual inspection of a levee stretch. Multiple groups surveyed the same part of the levee and every group found additional burrows that were missed by the other groups. The model described in this chapter aims to facilitate in this by attempting to quantify this uncertainty in manual inspection. Moreover, (Klerk, Kanning, Kok, Bronsveld, & Wolfert, 2021) did research on the Probability of Detection (PoD) of animal burrows and other levee slope discrepancies over 4 levee sections varying from 80 to 200 meters long. They concluded that the PoD of single animal burrow holes (described as 'damage points') was generally between 0.25 and 0.55. The report mentions that this low probability is partly caused by inspectors who usually do not take the effort to record every single animal burrow hole since this will take a large amount of time and the repair maintenance works usually cover the complete levee stretch anyway. However, the PoD for the burrowing section damage, describing the probability that the presence of animal burrows in the stretch is detected, varies from 0.5 to 0.8 (Klerk, Kanning, Kok, Bronsveld, & Wolfert, 2021). It can be concluded that the detection of animal burrow holes is inconsistent among inspectors and improvement of the probability of detection is desirable.

The input of the model should be based on different 'groups' of animal burrows that can initially be expected to be linked to each other after performing a first manual inspection. For example, if a full dike stretch of a couple of meters is inspected, and many burrow holes can be found in a proximity of each other, the smallest square around these burrows forms one group of burrow holes and the data from each separate group is the input for the model. This means that first a manual inspection should be performed that maps the location of all burrow holes found, these burrow holes should be formed into groups based on their relative locations and serve as the input for the model. This brings an uncertainty, since the identification of burrow groups is an objective process and can change from inspector to inspector. Furthermore, too small burrow groups will not lead to accurate predictions, so the main advice for identifying burrow hole groups is to only identify a group in case a clear split of multiple burrow holes from the 'crowd' is visible, as was the case in the data from chapter 5.2 with the vole burrow system. The parameters that should be taken from these groups and form the input of the model are the surface area that is covered by the burrow hole group and the amount of burrow holes in the group. The model then compares this values with the conclusions that were drawn from chapter 3.2, the following threshold values are set for the identification of burrow systems:

- If the surface area is smaller than 20 m^2, a vole burrow system is identified.
- If the surface area is larger than 90 m^2, a mole burrow system is identified.
- If the surface area is between 20 m^2 and 90 m^2, the density of the burrow holes is regarding to make a decision. This density is simply the ratio between the input amount of burrow holes and the input surface area:
    - If the density is larger than 2 burrow holes/m^2, a vole burrow system is identified.
    - If this ratio is smaller than 2 burrow holes/m^2, a mole burrow system is identified.

Upon identification of the burrowing animal, the expected amount of burrow holes in the input surface area is computed. This is done by the following steps:

1. The model chooses a random value for the distance between a burrow hole and the nearest burrow hole from the corresponding probability density function.
2. The surface area of a circle, with the distance drawn in step 1 as the radius, is calculated.
3. This surface area is subtracted from the input surface area and the model returns to step 1, drawing a new value for the distance until the total surface area is 'filled up' with circles.
4. The amount of burrow holes that fill up the surface area is counted and stored into a histogram.
5. Step 1 -4 is repeated a large number of times so that no significant changes in the distribution of the histogram is visible, let's assume 1000 iterations. In this way, the different possible combinations for the burrow hole distribution is simulated.
6. The model plots a cumulative distribution function through the data from the histogram that shows the randomly generated amount of burrow holes in the surface area, this function shows the probability that the amount of burrow holes in the surface area is less than a certain value.
7. The model returns the mean value for the expected amount of burrow holes and calculates the chance that the amount of burrow holes is larger than the input amount of burrow holes by using the cdf, so $P(X>A) = 1 - P(X<n)$, in which X is the expected amount of burrow holes and n is the input amount of burrow holes and $P(X<n)$ can be read from the plotted cdf.

In this way, the model can be used to assess the quality of the manual inspection and determine whether the inspector should further examine a certain stretch of the levee if the expected amount of burrow holes differs significantly from the amount of burrow holes that were found initially.

As the model bases its predictions on the small amount of data from the experiments that were carried out at LLHPP, the accuracy of the model could be improved by expanding the amount of data upon further research. Furthermore, the reliability of the model depends on how well certain burrow hole groups have been identified at first. In case this is done wrongly, and small burrow groups are falsely identified as vole burrow systems, this will lead to incorrect predictions. It can be concluded that while the model is sensitive to errors in this way, it can serve as a useful tool that can help during the manual inspection of levees.

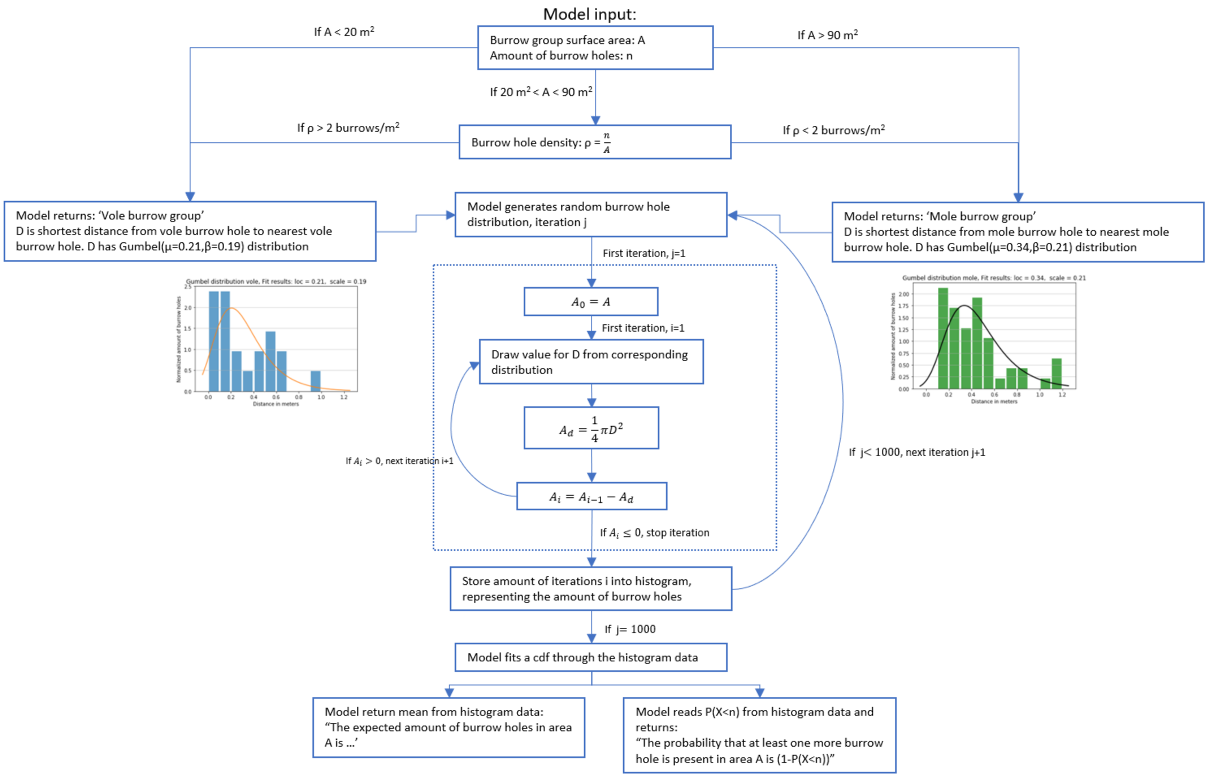

Figure 42: Proposed procedure of levee inspection probabilistic model

Figure 42 shows the procedure that the model would follow, in which j represent the iterations of generating a random burrow hole distribution and i represent the iterations of drawing a value for the distance from one burrow to the nearest burrow and subtracting its area from the total surface area. Both i and j are integers, starting with a value of 1.
For example, if the inspector finds 20 burrow holes over a surface area of 40 m^2, the model will identify it as a mole burrow system based on the burrow hole density. If the randomly generated burrow distributions show an expected amount of burrow holes of 75, the inspector can conclude that additional inspection is necessary over this stretch. On the other hand, if the inspector find 60 burrow holes over the same surface area of 40 m^2 and the model predicts 75 burrow holes to be present, the inspector could decide that his inspection is sufficiently accurate. It has to be noted here that the guidelines for these decisions are not clear and mainly depend on the experience of the inspector. In other words, it is unknown and therefore not taken into account for what percentage of found burrow holes the inspection can be deemed as sufficiently accurate.

The model initially only bases the identification of a mole or vole burrow system on the input area of the burrow group, only when the value of the area is between 20 m^2 and 90 m^2, the burrow hole density will be taken into account as well. In practice however, this will lead to incorrect predictions in cases where a string of linear burrow holes is found. As described in chapter 3.1, moles tend to dig linear corridors, which is also found during earlier experiments at the LLHPP (Tsimopoulou & Koelewijn, 2022), where several burrow holes where found in a nearly vertical distribution. In these cases, the area of the smallest square around the burrow holes will be small and the model will incorrectly identify it as a vole burrow system. Furthermore, the robustness of this step of the model, the identification of the responsible animal, could be improved in general.
In order to do so, a small logistic regression model is developed in addition to the probabilistic model that also takes the linearity of the burrow holes into account. Logistic regression is otherwise known as binary classification, as it models a binary outcome: something is either true or false (Brannick, sd). We use the characteristics from the burrows found during the experiment to set this up. For instance, when looking at the surface area of the identified burrows, we assign a value of '1' to the surface areas that are found for the mole burrows and a value of '0' to the surface areas of the vole burrows. When plotting this, the graph will look like the one in Figure 43. It has to be noted that graph in Figure 43 doesn't represent the actual data from the experiments, it is merely an illustration to explain the procedure of the logistic regression model.

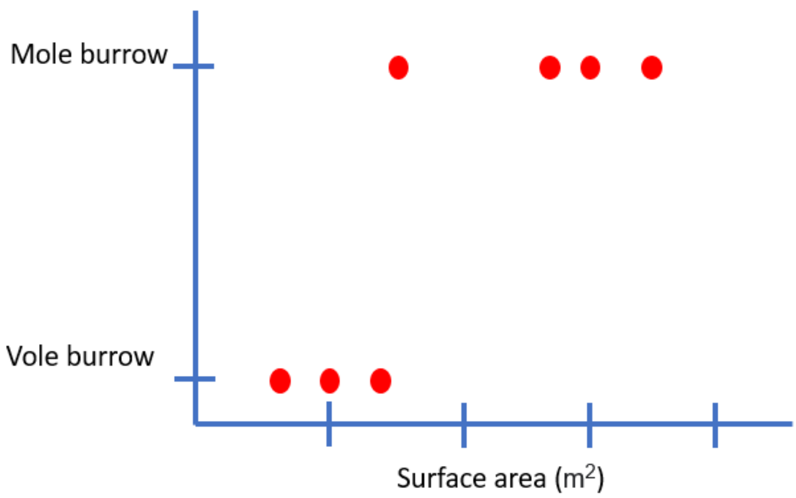

Figure 43: Example of binary classification of burrows based on surface area.

The model will then fit a logistic function in the form of: $P(x) = \frac{1}{1+e^{-(x-\mu)/s}}$, where µ is the location parameter and s is the scale parameter . The model takes the maximum likelihood values for µ and s and plots the function, as illustrated in figure 44. Whenever a new burrow group is found, the value of the surface area X corresponds to a probability P(X), in case this probability is larger than 0.5, the model will identify the burrow group as a mole burrow, if P(X) < 0.5, the burrow group is identified as a vole burrow.

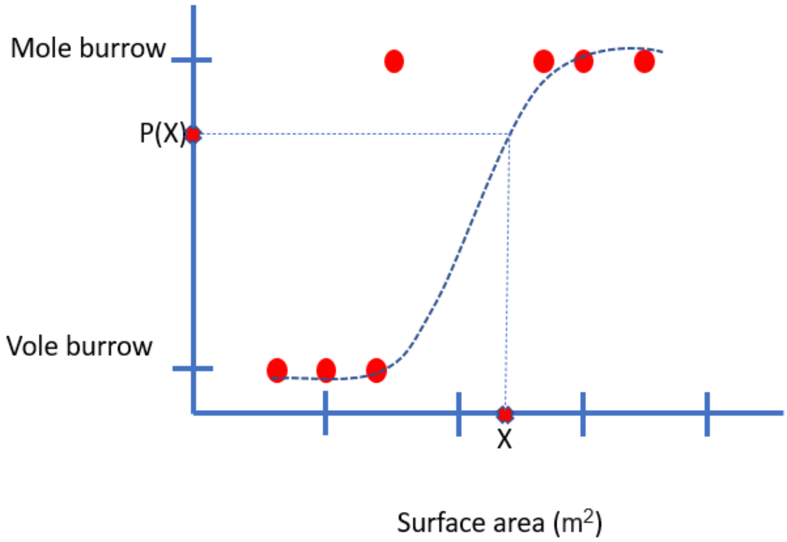

Figure 44: Illustration of how binary classification works in practice.

As is the case with the original probabilistic model, there is simply not enough data to fit a representative logistic function through the data points. The values for the parameters µ and s have been manually chosen based on the conclusions that could be drawn from the experiment data in combination with several assumptions. It is recommended that more data is collected such that the assumed values for these parameters can be adjusted or verified.

Apart from the surface area, a logistic function is fitted for the burrow hole density. Furthermore the ratio between the shortest dimension of the burrow area and the longest dimensions of the burrow area, describing the linearity in the burrow holes, is taken into account as well. A factor β is introduced, which is equal to $\beta = 1 - \frac{\min(H,W)}{\max(H,W)}$, where H is the height of the burrow area in meters and W is the width of the burrow hole area in meters. The value for β can be between 0 and 1, where β=0 corresponds to a square burrow hole area, which hints towards a vole burrow system since they are characteristically less linear than mole burrows. Towards the extreme case of β=1, the burrow area shows a more slender, linear shape which hints towards a mole burrow system. However, linear systems under an angle, so not exactly horizontal or vertical, can still have a low value of β and therefore falsely be identified as a vole burrow system. This is why another parameter is taken into account in the logistic regression model, namely the value of r^2 , which is the square of the correlation coefficient r, describing the correlation between the x-coordinate and y-coordinate of the burrow hole. In our model, it describes how well all the burrow holes are located on the line that is fitted through the burrow holes during a linear regression fit. The value of r^2 can be between 0 and 1, a high value describes a linear burrow hole distribution, hinting towards a mole burrow system.

As previously mentioned, the values of the location and scale for each of the 4 parameters are manually determined and the results can be seen in figure 45.

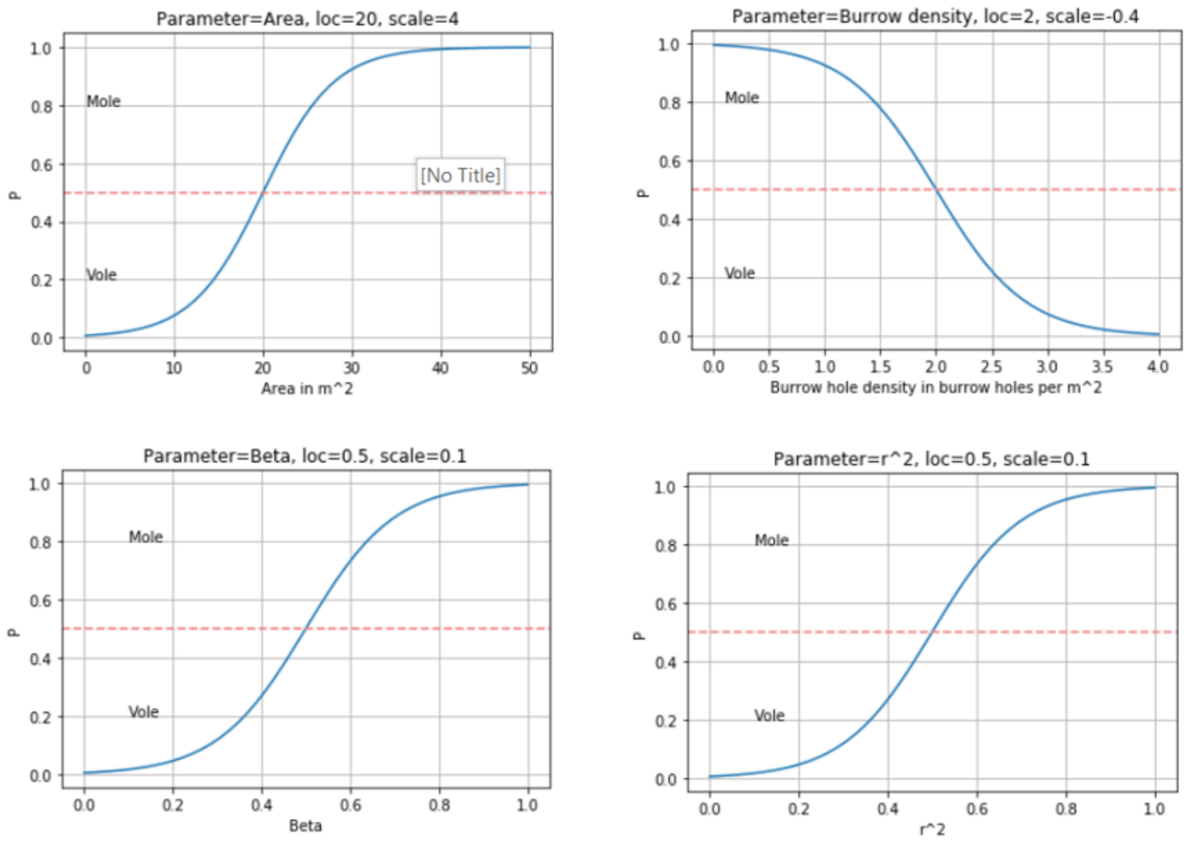

Figure 45: Logistic regression fits for each of the parameters

In Figure 45, the location parameters for the area and burrow density parameters have been chosen based on the guidelines from chapter 3 and chapter 5. For the beta and r^2 parameters, these values have been set at 0.5, thus assuming that surface areas where the width is twice the value of the height or vice versa for Beta distinguishes a mole burrow system from a vole burrow system.

In order to determine a final classification, the weighted average of each of the probabilities for the 4 parameters is taken. The importance of area and burrow hole density are assumed to be most significant and are therefore assigned a weight of 35% each. The value for beta and r^2 are given a weight of 15% each, where it has to be noted that the distribution of these weights leave room for discussion and further research into this is required. All in all, the final value for the binary classification model P_{tot} can be calculated in the following way:

$$P_{tot} = 0.35 * P_{area} + 0.35 * P_{density} + 0.15 * P_{\beta} + 0.15 * P_{r^2}$$

Where the value of each $P_{parameter}$ follows from the respective logistic regression curve from Figure 45. This model, from which the python script can be found in Appendix D, can now be tested by using the coordinates from the vole and mole burrow holes from chapter 5 and plotting the results, as visible in Figure 46.

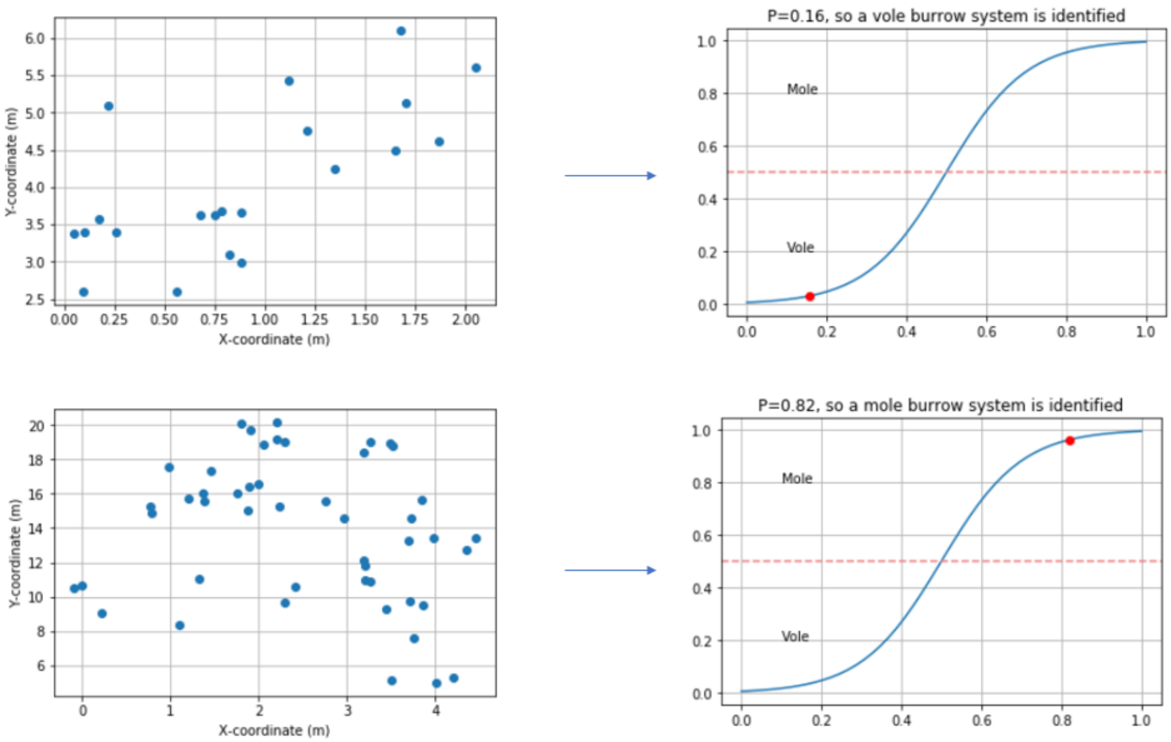

Figure 46: testing the logistic regression model for the vole (top row) and mole (bottom row) burrow data

Figure 46 shows that the model correctly identifies the responsible animal for the burrowing. While the model is based on a lot of assumptions that stem from a small sample size, it can be used as a first indication to identify the animal that created the found burrow hole by only using the coordinates of the burrow holes as input. Further research is required to gather additional data that can verify or change the values for the location and scale parameters that are used for the logistic curve and the weights that are assigned to the various parameters.

Chapter 7: Conclusions, discussion and recommendations

The first phase of this report aimed to answer the following research question: 'How do animal burrows influence dike performance?' and it aimed to form a foundation for the second phase of the report by focusing on the behavior of burrowing animals and the geometrical characteristics of their burrows. It was found that animal burrows influence levee performance in a number of ways. First of all, extensive animal burrowing will change the hydraulic conditions of the levee, increasing the probability of piping, micro-instability or macro-instability to occur. This is caused by animal burrows that tend to penetrate deep into the levee body, for example those made by muskrats. Secondly, the erosion resistance in case of overtopping is strongly reduced by the presence of animal burrows inside the surface of the inner levee slope. Finally, collapse of animal burrows can lead to a reduction of the crest height, potentially leading to more overtopping and overflow during high water.

In practice, the large animal burrows and the responsible animals are easily identified since they all have distinct characteristics and since large burrows pose a higher risk for levee safety, active prevention of these burrow holes in and around levees is applied. However, the smaller burrow holes made by voles and moles show identical characteristics regarding location, size and depth. In practice, the identification of these burrows rely on the assessment and experience of the levee inspector. Available literature suggest that the main difference between these burrow systems is the burrow size and burrow hole density. Mole burrow systems can be several hundred square meters, while vole burrow systems rarely surpass 20 m^2. Furthermore, research has indicated that vole burrow system show more than 2 burrow holes per square meter of surface area while mole burrow systems do not and mole burrow hole distributions have shown to have a more linear character as opposed to often randomly distributed vole burrow holes.

These conclusions could then be used to identify different vole and mole burrow hole groups in data that was collected from several experiments at the Living Lab Hedwige and Prosper Polder (LLHPP) and answer the research question for the second phase, which was: 'Based on data from levee inspection experiments, which probabilistic model can contribute to the manual inspection of animal burrows?
'. During the analysis of the experiment data, it was concluded that smoke experiments can potentially serve as a quick and effective method to gain insights in the connectivity between burrow holes and discover new burrow holes that are otherwise hard to discover by the naked eye.

The aim of the aforementioned probabilistic model is to identify which animal was responsible for the burrow based on input parameters, which are the surface area covered by the burrow group and the amount of burrow holes within the group, that are collected during manual inspection of the levee and assess the quality of this inspection based on the expected amount of burrow holes within the input surface area. Since currently no guidelines for levee inspection exist other than the opinion and experience of the levee inspector, the model aims to facilitate the manual inspection of a levee.

This probabilistic model was constructed by collecting the data from the experiments regarding the distance from each burrow hole to the nearest burrow hole for both vole burrows and mole burrows, fitting probability density functions through them and letting the model generate random burrow hole distributions for the input surface area. Analysis performed on the experiment data suggests that a Gumbel distribution best fits the data in both vole and mole burrow systems. More specifically, it was concluded that the probability density function for the shortest distance from a vole burrow to the nearest vole burrow can be described by a Gumbel(μ=0.21,β=0.19) distribution and the probability density function for the shortest distance from a mole burrow to the nearest mole burrow can be described by a Gumbel(μ=0.34,β=0.21) distribution. Where μ is the location parameter and β is the scale parameter.

In addition to this, a logistic regression model is developed in order to identify the responsible burrowing animal taking more parameters into account than was originally done in the probabilistic model. These parameters were, besides the surface area and burrow hole density, the factor β which describes the 'slenderness' of the surface area and thereby taking the linearity in burrow hole distribution into account. Finally, the value of r^2, with r being the correlation coefficient of a linear regression fit through the burrow holes. This parameter also acts a indication of how well all the burrow holes fit on one line, high values for β and r^2 both hint towards mole burrow systems. The logistic regression model then takes a weighted average of the binary classification probability, if a value of 0.5 or higher is returned, a mole burrow hole is identified. In this way, inspectors can get a quick insight into the responsible burrowing animal and he/she can take further action.

The results from this thesis can be useful for manual inspection of the levee surface as it is known to be hard to find all the burrow holes on a levee surface. After an initial inspection of the levee stretch, the locations of the found burrow holes should be mapped and the inspector should look for distinctive burrow groups and/or patterns. The input parameters should be entered into the model which returns the responsible burrowing animal, from which a few conclusions regarding the spatial distribution of the burrow holes can already be drawn. For example, if a group is identified as a vole burrow system based on the input parameters, the inspector should conclude that more burrow holes can potentially be found within a short range of a few meters within the found burrow hole group, whereas burrow holes of a mole burrow system can be found all over the levee surface. Identification of a mole burrow system from the logistic regression model could mean that the burrow holes will extend further throughout the levee and the inspector could choose to conduct additional survey to find the remaining burrow holes. Furthermore, the probabilistic model returns the expected amount of burrow holes within the input surface area and the probability that at least one more burrow hole is present. These output parameters can be used to interpret whether additional inspection is necessary in case of a large discrepancy between the found amount of burrow holes and the expected amount of burrow holes.

It has to be mentioned that all the key conclusions in this report have been made based on a small amount of data. Firstly, the conclusions regarding the threshold value for the difference in burrow size between vole and mole burrow systems in chapter 3 have been based on a single report that recorded the size of 50 vole burrow systems in Switzerland. This is a small sample size which could mean that the discovered characteristics might be relatively unique and therefore lead to unrealistic depictions when applied on broader scale. The effect of the difference in soil characteristics that are present at the research site in Switzerland and the typical levee soil conditions have been neglected as well. Similarly, the characteristics for mole burrow systems that are used in this report to identify mole burrows stem from a research on merely 15 mole burrow systems in 1969, therefore neglecting any possible changes in mole behavior and measurement techniques over the years. It can be concluded that the guidelines which are used throughout this report to identify mole and vole burrow system from the experiment data and in the probabilistic model, are based on a small sample size.
On top of that, the data from the experiments that have been carried out at the LLHPP only include 93 burrow holes that have been sorted into two burrow groups, one vole burrow group and one mole burrow group. The vole burrow group only contains 24 burrow holes, from which it is hard to draw definite conclusions. Ideally, conclusions are drawn from a few hundred data points but the relatively small size of the experiments did not allow for this. This leads to bad fits in the distribution functions for both the vole and the mole 'nearest burrow'-histograms, eventually the least-worse distribution is chosen based on visual interpretation combined with the fact that Gumbel-distributions are usually applied in extreme-value analyses, like a shortest-distance plot. For the logistic regression model, the lack of sufficient data leads to manually determined values for the location and scale parameter in the fitted logistic function, whereas they are ideally determined from experiment data as the value for the parameters with the maximum likelihood. By manually choosing these values, the accuracy and reliability of the logistic regression model is reduced and for further research, it is recommended that the chosen values are validated or adjusted using a sufficient amount of burrow group data.
In chapter 5, where the RTK coordinates are transformed into the local coordinate systems, a number of assumptions have been made regarding the orientation of the levee. For example, the angle of the levee with respect to the Rijksdriehoek coordinate system was computed using a protector which can

lead to inaccuracies as it is manually read and rounded off. Since the value for the Rijksdriehoek coordinates are in the order of several thousand meters, a small discrepancy in this angle can lead to a significant error in the local coordinate system. Therefore, it is very possible that the locations of these data points are incorrect by a margin of a few decimeters. The same can be said about the levee slope angle, which is derived from manually reading measurement from ahn.nl. In reality, a different slope angle might be present, which again has consequences for the local y-coordinates of the RTK points.

In this report, the results from the grouting and smoke experiments are collected and used to derive the characteristics of the vole and mole burrow systems. However, the accuracy of these detection methods could not be determined in this research, since no part of the 4 meter wide levee that formed the experiment site was tested by all the detection methods (grouting and excavation, smoke testing and GPR scanning). It was concluded that smoke testing can potentially contribute to manual inspection of a levee, since it is a fast way to get insight in the connectivity between nearby burrow holes compared to the other techniques that require a long waiting time (in case of grouting) and/or an amount of data processing and interpretation (in case of GPR scanning). However, the accuracy of the smoke experiments could not yet be determined, therefore it is unknown what percentage of connected burrow holes can be detected using this technique, how far the smoke will travel up the burrow system and other characteristics. It is recommended that these experiments are carried out again on a ‘fresh’ levee stretch where careful attention is paid to the overall distribution of the burrow holes and their locations. In the experiments that were described in chapter 4, no clear records were made of what experiments had previously been carried out at what part of the levee stretch. For the new experiments, the following recommendations can be made to enhance the data collection and analysis and prevent confusion regarding the locations of the burrow holes.

- The exact locations of the burrow holes that are found during an initial manual inspection should be carefully mapped using a local grid system. This can potentially be done in a similar way as the grid that was used during the GPR scanning described in chapter 4.1.2, consisting of grids with a width of 50 centimeters and a length of 1 meter.
- Marking the origin of this local coordinate system and making sure it can clearly be found (for example by marking it with spray-paint, taking pictures of the surroundings or accurately describing it in words) is essential, since the experiments are likely to be spread over multiple days. In this way, the local grid can quickly be built up again and the previously found burrow holes can easily be detected from the map.
- Indicate, based on the spatial distribution and the knowledge regarding the system characteristics, where vole burrow systems could potentially be present, choose the lowest burrow hole of this group to start blowing smoke into the vole burrow system.
- Indicate which burrow holes are likely part of a mole burrow system and choose the lowest point to conduct another smoke experiment.
- Use a piece of plywood to cover the burrow holes that showed smoke during the experiment, if needed a waterproof marker can be used to indicate the order in which the burrow holes started to show smoke, which burrow system the hole is part of or other relevant information. The aim of this is to gain insight in how the smoke will travel up the burrow tunnels and to avoid confusion during the processing of the data.
- Fill up the burrow holes that were part of the smoke experiments with grout and record the amount of grout that was poured into each hole. Also mark the locations of the burrow holes that were used as the ‘starting points’ of the grouting procedure.
- For the GPR scanning, clearly identify which burrow holes are grouted and are therefore of interest to be scanned.
- When collecting RTK coordinates, photograph every point that is scanned and give the corresponding data point a clear name. A recommendation for the name is the local coordinates of the point, this way a translation from the Rijksdriehoek to the local coordinate

system no longer depends on the assumptions that were made in this report. By taking photographs, registration of the LiDAR scans is simplified.

By following these recommendations, it is ensured that the different detection methods can be compared as the grouted burrow systems that were also scanned with the GPR scanner and were subjected to the smoke experiment can be excavated. The excavations can form the reference to assess the accuracy of the GPR scans and the smoke tests. Further research can focus on the applicability and accuracy of these detection methods to further improve the efficiency of manual inspection of levee surfaces.

All in all it can be concluded that the effects of shallow animal burrows on levees created by small animals like voles and moles are currently not taken into consideration when designing or assessing a levee while it has a significant impact on the erosion resistance of the inner slope in case of overtopping or overflow during high water. Furthermore, no guidelines for assessing the severity of animal burrows on the levee slope exist except for the experience of the levee inspector. In order to develop such guidelines in the future, accurate manual inspection of a levee slope is required. This report has suggested that using a probabilistic model which uses data regarding the spatial distribution of animal burrow holes to identify the responsible burrowing animal and estimate the extent of the underground burrow system is possible, however more data by performing more experiments is necessary to improve the quality of the fitted distribution function as well as to assess the accuracy of the detection methods that were used to retrieve the data and possibly improve the efficiency of manual levee slope inspection. This can provide crucial information towards quantification of the effect of animal-induced levee anomalies in the future.

Appendix A: Burrow hole grouting data

Table A.1 shows the exact location of the grouted burrow holes as well as the diameter of the burrow hole and the depth of the burrow hole. The burrow holes which are marked as 'grouted on 7-10-2021' represent burrow holes that were part of excavations on October 9th 2021, in the map in Figure A.2 these points are marked with green. For the smoke experiment burrow holes, the remarks show the amount of grout poured into each burrow. The x- and y-coordinates represent the coordinates of the burrows in the local coordinate system, with the origin being at the edge of the asphalt road in the top left of the 4 meter wide levee stretch.

Table A.1: Exact location, depth and diameter of grouted burrow holes

	X (m)	Y (m)	depth (cm)	Diameter (cm)	Remarks
1	0.09	2.6	28	4	grouted on 7-10-21
2	0.56	2.6	27	2	grouted on 7-10-21
3	0.88	2.98	10	3	grouted on 7-10-21
4	0.82	3.1	22	3	grouted on 7-10-21
5	0.05	3.38	20	2	grouted on 7-10-21
6	0.1	3.4	9	2	grouted on 7-10-21
7	0.26	3.4	11	2.5	grouted on 7-10-21
8	0.17	3.57	15	3	grouted on 7-10-21
9	0.68	3.62	17	3	grouted on 7-10-21
10	0.75	3.62	5	2	grouted on 7-10-21
11	0.78	3.68	22	1.5	grouted on 7-10-21
12	0.88	3.66	10	1.5	grouted on 7-10-21
13	1.35	4.25	16	4	grouted on 7-10-21
14	1.65	4.5	20	3	grouted on 7-10-21
15	1.87	4.62	20	3.5	grouted on 7-10-21
16	1.21	4.75	19	6	grouted on 7-10-21
17	4.01	5	23	2.5	direction: almost parallel to the slope grouted on 7-10-21
18	0.22	5.1	20	2	grouted on 7-10-21
19	1.7	5.13	21	4	grouted on 7-10-21
20	3.5	5.14	17	3	grouted on 7-10-21
21	4.2	5.27	23	3	grouted on 7-10-21
22	1.12	5.43	17	3	grouted on 7-10-21
23	2.05	5.6	19	3	grouted on 7-10-21
24	1.68	6.1	22	2	
25	3.76	7.6	13	2	
26	1.1	8.33	16	2	
27	0.22	9.05	29	4.5	
28	3.45	9.25	15	4	
29	3.86	9.5	7	2	
30	2.3	9.7	26	1.5	
31	3.71	9.74	11	3	
32	-0.09	10.5	32	2	connected with point 33
33	0	10.65	21	3	connected with point 32
34	2.42	10.58	17	2.5	
35	3.26	10.87	16	3	
36	3.21	11	21	2	
37	1.33	11.05	17	3	

38	3.2	11.85	13	2	
39	3.19	12.13	15	2	
40	4.35	12.7	24	2	
41	3.7	13.3	12	2	
42	4.45	13.39	26	2	
43	3.98	13.45	12	1.5	
44	2.97	14.55	13	2	
45	3.72	14.55	25	2	
46	0.79	14.9	13	3.5	
47	1.88	15	39	3	
48	0.77	15.3	17	3	
49	2.24	15.3	15	3	
50	1.39	15.55	16	3	
51	2.75	15.55	21	3	
52	3.85	15.64	35	2.5	
53	1.2	15.76	16	3	
54	1.75	16.03	15	2.5	
55	1.37	16.06	13	2	
56	1.89	16.43	30	3	
57	1.99	16.55	29	3	
58	1.46	17.3	17	3	
59	0.98	17.6	22	3	
60	3.19	18.38	19	5	this is a squared hole, artificially made.
61	3.52	18.78	18	2.5	
62	3.49	18.93	26	2	
63	3.27	19.02	37	3	
64	1.8	20.1	14	3	
65	2.2	19.2			
66	2.3	19.05			
67	2.05	18.9			
68	1.9	19.7			
69	2.2	20.15			
70	2.8	14.7			Grout poured into this hole
71	0.7	15.1			Took 0.5L of grout, marked 'A'
72	0.7	15.5			Took 0.5L of grout, marked 'B'
73	1.1	15.8			Marked with 'C'
74	1.35	15.8			Marked with 'D'
75	1.35	16.05			Marked with 'E'
76	1.7	16.15			
77	1.9	16.6			Marked with 'F' / (or 'I'?)
78	2.05	16.75			marked 'g', took 7L of grout
79	1.6	17.3			marked 'K'
80	1.1	17.8			marked 'L', smoke start
81	3.8	15.9			
82	3.35	18.9			marked 'X', took 0.5L of grout, exact location unsure
83	3.65	19			marked 'Y', took 6L of grout, exact location unsure

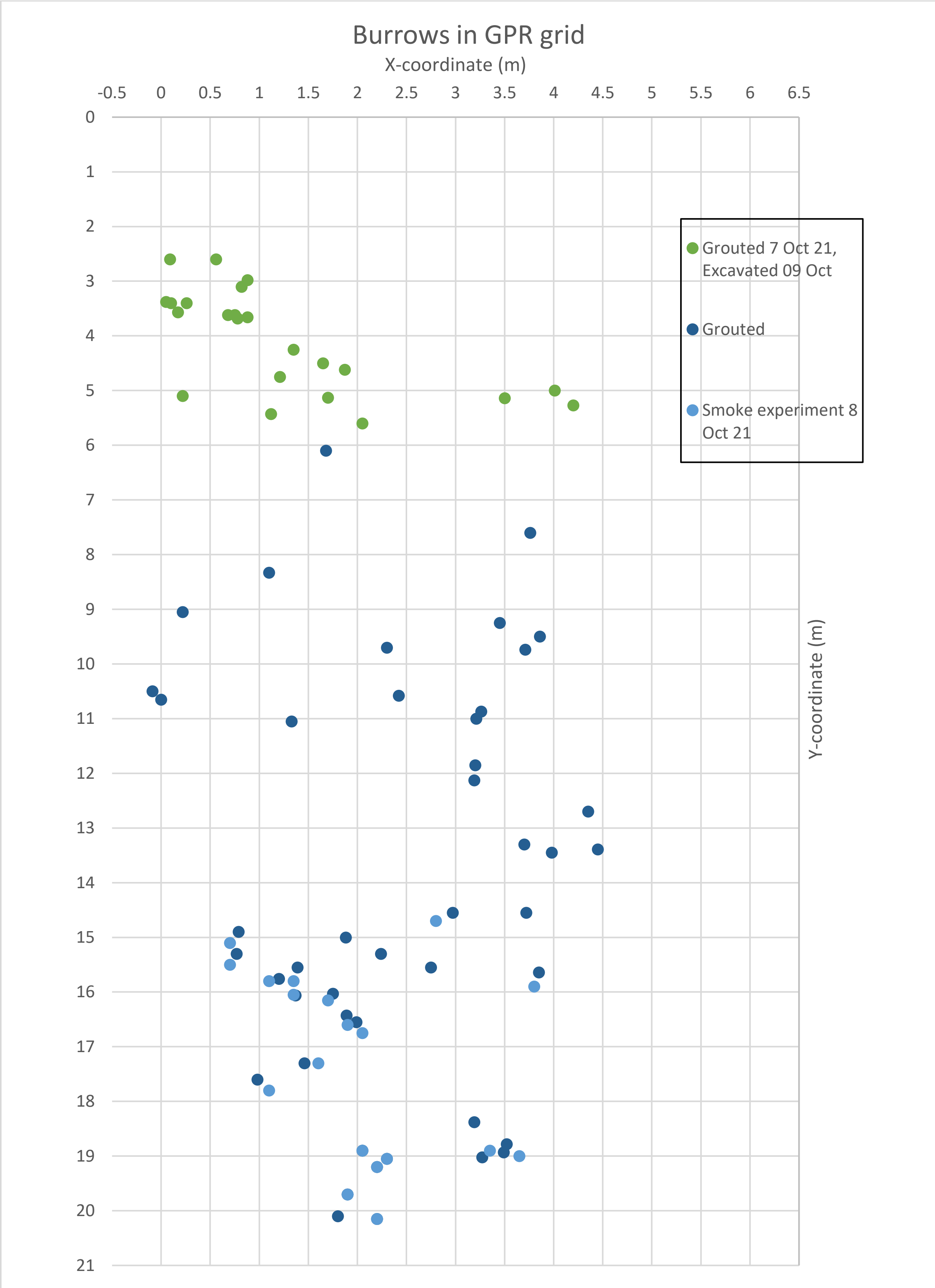

Figure A2: Complete burrow map

Appendix B: Excavation pictures

This appendix displays additional pictures that have been taken of the excavated mole burrow tunnel from excavations on February 9th 2022. The excavated part of the main linear tunnel, from which multiple branches have been found to be connected, spans a length of a nearly 3 metres but is expected to extend all throughout the levee surface, as described earlier in Chapter 5.2.

Figure B1: Overview of excavated tunnel, numbers indicate location of detailed images

Figure B2: Overview of excavated tunnel, numbers indicate location of detailed images

Figure B3: Tunnel leading towards burrow hole that showed grouted pouring out, labelled as 1 in Figure B1

Figure B4: Two branches near each other, labelled as 2 in Figure B1

Figure B5: Tunnel curve, labelled as 3 in Figure B1

Figure B6: Tunnel junction, branching off towards the surface, labelled as 4 in Figure B1 and Figure B2

Figure B7: Fragments, making up a linear tunnel. Labelled as 5 in Figure B2

Figure B8: Tunnel branch heading further into the soil, labelled as 6 in Figure B2

Appendix C: Python script probabilistic model

This chapter shows the python script that is used to compute the histogram for the shortest distance from each burrow hole to the nearest burrow hole.

```
In [11]: def find_len(list1): #function that returns the second smallest value in a list,
                             #so that the distance from each burrow to the burrow itself is ignored
             length = len(list1)
             list1.sort()
             return list1[1]
```

```
In [12]: volex = (0.09,0.56,0.88,0.82,0.05,
         0.1,0.26,0.17,0.68,0.75,0.78,0.88,1.35,1.65,1.87,1.21,0.22,1.7,1.12,2.05,1.68) #x-coordinates vole burrows
         voley = (2.6,2.6,2.98,3.1,3.38,3.4,3.4,3.57,3.62,3.62,3.68,3.66,4.25,4.5,4.62,4.75,5.1,5.13,5.43,5.6,6.1,) #y-coordinates vole bu
         A = np.zeros(len(volex))
         for i in range(len(A)):#goes through the coordinates and takes each one as the base points
             xbase,ybase = volex[i],voley[i]
             distances = np.zeros(len(A))
             for j in range(len(A-1)): #computes the distance from each basepoint to every other point
                 if j==i:
                     continue
                 else:
                     distances[j]=np.sqrt(((xbase-volex[j])**2)+((ybase-voley[j])**2)) #equation to calculate the value of the distance
             A[i]=find_len(distances)
```

Figure C1: Python script used for shortest distance to nearest burrow.

Appendix D: Python script logistic regression model

This chapter shows the python script that is used to compute logistic regression model, as visible in Figure D1. Behind the code lines, further information regarding the process of the model can be found.

```
#Enter coordinates
xcoordinates= np.random.rand(10)*1 #Array containing x-coordinates
ycoordinates= np.random.rand(10)*2 #Array containing y-coordinates

#Plotting the burrow holes
plt.plot(xcoordinates,ycoordinates, 'o', label = 'points')
plt.grid()
plt.ylabel('Y-coordinate (m)')
plt.xlabel('X-coordinate (m)')
```

```
def LogisticReg(xcoordinates,ycoordinates):
    #The model computes the parameters based on the input coordinates
    Width = np.max(xcoordinates)-np.min(xcoordinates)
    Height = np.max(ycoordinates)-np.min(ycoordinates)
    Area = Width * Height
    beta = 1 - (np.min([Width,Height])/np.max([Width,Height])) #the ratio between height and width
    nburrow = len(xcoordinates) #Amount of burrow holes
    density = nburrow / Area
    line = linregress(xcoordinates,ycoordinates) #fitting a straight line through the burrow holes to evaluate the value of r^2
    r2 = line[2]**2

    #Binary classification for every parameter
    Pa = 1/(1+np.exp((-(Area-20))*0.25))      #Area
    Pden = 1/(1+np.exp((-(2-density))*2.5))  #density
    Pr2 = 1/(1+np.exp((-(r2-0.5))*10))       #Linearity
    Pbeta = 1/(1+np.exp((-(beta-0.5))*10))   #Height/width ratio

    #Assigning weight to the parameters
    weighta = 0.35                            #Area
    weightden = 0.35                          #density
    weightr2 = 0.15                           #Linearity
    weightbeta = 0.15                         #Height/width ratio

    #Computing the value for P and performing final Binary classification
    P = weighta*Pa+weightden*Pden+weightr2*Pr2+weightbeta*Pbeta
    if P>=0.5:
        result= f'P={P:.2f}, so a mole burrow system is identified'
    else:
        result= f'P={P:.2f}, so a vole burrow system is identified'

    #Plotting the results
    Y=1/(1+np.exp((-(P-0.5))*10))
    Xp=np.linspace(0,1)
    Yp=1/(1+np.exp((-(Xp-0.5))*10))
    plt.plot(Xp,Yp)
    plt.plot(P,Y,'o',color='r',)
    plt.grid()
    plt.title(result)
    plt.axhline(y=0.5,ls='--',color='lightcoral')
    plt.text(0.1,0.8,f'Mole')
    plt.text(0.1,0.2,f'Vole')
    return
```

Figure D1: Python script for logistic regression model

References

AHN.nl. (2022). *AHN viewer*. Retrieved from Website of AHN: https://www.ahn.nl/ahn-viewer

Bayoumi, A., & Meguid, M. A. (2011). *Wildlife and Safety of Earthen Structures: A Review.* Springer.

Brannick, M. (n.d.). *Logistic Regression*. Retrieved from http://faculty.cas.usf.edu/mbrannick/regression/Logistic.html

Brügger, A., Nentwig, W., & Airoldi, J.-P. (2010). *The burrow system of the common vole (M. arvalis, Rodentia) in Switzerland.* Bern: University of Bern.

Cobos-Roa, D. A. (2015). *Transient Seepage Through Levees and the Influence of Roots and Animal Burrows.*

Deltares. (2014). *Onderzoek naar muizenschade in keringen in Fryslân.* Delft.

DoubleRoot. (2022). *Rotation of Axes*. Retrieved from DoubleRoot website: https://doubleroot.in/lessons/coordinate-geometry-basics/rotation-of-axes/

FEMA. (2005). *Impacts of Animals on Earthen Dams.*

Google Maps. (2022). *Google Maps*. Retrieved from Google Maps website: https://www.google.nl/maps/@51.3427826,4.2367665,15.44z

GPRS. (2022). *GPR explained*. Retrieved from https://www.gp-radar.com/article/gpr-explained

Haeck, J. (1969). *Colonization of the mole in the IJsselmeer polders.* Arnhem: Netherlands Journal of Zoology.

Hoogheemraadschap De Stichtse Rijnlanden. (2020). *Muskusrattenbeheer*. Retrieved from Veilige dijken: https://www.hdsr.nl/werk/veilige-dijken/muskusrattenbeheer/

Jonkman, S., Steenbergen, R., & Morales-Nápoles, O. (2017). *Probabilistic Design: Risk and Reliability Analysis in Civil Engineering.* Delft.

kadaster.nl. (2022). *Rijksdriehoeksstelsel*. Retrieved from kadaster.nl website: https://www.kadaster.nl/zakelijk/registraties/basisregistraties/rijksdriehoeksmeting/rijksdriehoeksstelsel

Kennis- en Adviescentrum Dierplagen. (2022). *Dierplagen*. Retrieved from Kennisbank: https://www.kad.nl/kennisbank/dierplagen/

Klerk, W., Kanning, W., Kok, M., Bronsveld, J., & Wolfert, A. (2021). *Accuracy of visual inspection of flood defences.* Structure and Infrastructure Engineering.

Koelewijn, A., Kieftenburg, A., & Hûsken, L. (2020). *Graverij door dieren.* Delft.

Laundré, J., & Reynolds, T. (1990). *Burrows and burrowing behaviour by mammals.* New York, London: Plenum Press.

Mellanby, K. (1971). *The Mole.* William Collins Sons & Co Ltd.

Palladino, M. e. (2019). *Impact of animal burrows on earthen levee body vulnerability to seepage.* Wiley.

Provinsje Fryslân. (2015). *Muizenplagen in Nederland.*

STOWA. (2022). *Plaagsoorten in en op de dijk (PIW)*. Retrieved from STOWA website: https://www.stowa.nl/onderwerpen/waterveiligheid/inspecteren-beheren-en-onderhouden/plaagsoorten-en-op-de-dijk-piw

Tsimopoulou, V., & Koelewijn, A. (2022). *Animal burrows survey on the Hedwige Levee (8th September 2021).* Delft.

Utiugova, O. (2021, July 22). *Introduction to RTK GNSS*. Retrieved from Emlid: https://emlid.com/introduction-to-rtk-gps/

Van Baars, S. (2009). *The Causes and Mechanisms of Historical Dike Failures in the Netherlands.* Delft: European Water Association.

Waterschap Rivierenland. (2020). *Beverprotocol*. Retrieved from Waterschap Rivierenland website: https://www.waterschaprivierenland.nl/beverprotocol

YPTE. (2021). *Mole Habits*. Retrieved from YPTE website: https://ypte.org.uk/factsheets/mole/mole-habits

Zoogdiervereniging. (2021). *Konijn*. Retrieved from Zoogdiervereniging web site: https://www.zoogdiervereniging.nl/zoogdiersoorten/konijn